Morales-Cespedes, M., Vandendorpe, L. & Armada, A. G. (2021). Interference Management for K-Tier Networks Without CSIT Based on Reconfigurable Antennas. *IEEE Transactions on Communications, 69*(12), 8068–8084.

DOI: 10.1109/tcomm.2021.3116246

# Interference Management for $K$-Tier Networks without CSIT based on Reconfigurable Antennas

Maximo Morales-Cespedes, *Member, IEEE*, Luc Vandendorpe, *Fellow, IEEE*, Ana Garcia Armada, *Senior Member, IEEE*

***Abstract*—Heterogenous networks are mainly limited by interference. Nowadays, the advances in reconfigurable antennas allow us to implement blind interference alignment (BIA) schemes, which avoid the need for channel state information at the transmitter (CSIT) while providing an increasing multiplexing gain, i.e., the achievable DoF, as the number of users increases. In this work, we propose a downlink transmission scheme based on BIA for managing the inter-tier interference in $K$-tier networks, referred to as tier BIA (tBIA). The tBIA scheme can be implemented considering that each tier employs any BIA scheme for managing the intracell and intercell interference. In this sense, considering proper BIA schemes applied to each tier, tBIA fully cancels all the sources of interference. After that, the DoF outer-bound for $K$-tier networks without CSIT is derived. It is shown that tBIA reaches this outer-bound. Furthermore, it is demonstrated that fully managing the inter-tier interference provides larger DoF in the whole network than turning off any tier with the aim of improving the achievable DoF in the remaining tiers. Simulation results show that the proposed tBIA scheme provides greater DoF and improves the user rates in comparison with other schemes without CSIT in multi-tier networks.**

***Index Terms*—Heterogeneous Networks, Reconfigurable Antennas, Blind Interference Alignment, Degrees of Freedom, Channel State Information.**

## I. Introduction

Interference is the main limitation in heterogeneous networks [1]. During the last decade, the transmission power of the base stations (BSs) has been adapted, increasing or decreasing, in order to improve the area spectral efficiency [2]. As a consequence, the cellular networks become more heterogeneous and composed of several tiers. Consequently, the interference management in the future networks needs to handle a extremely dense and heterogeneous deployment of BSs arranged in several tiers interfering among them.

The general $K$-tier downlink network is analyzed in [3] using stochastic geometry tools for determining the distribution of both BSs and users. It is shown that the coverage probability does not depend on the number of tiers. Moreover, in [3], each user is associated to the tier in which the BS that provides the highest signal-to-interference ratio (SIR) is located as is shown in Fig. 1(a). Taking into consideration load balancing among BSs, an alternative user association is proposed in [4]. Considering the utility of the whole network, the optimality of the tier selection and user association is analyzed in [5]. It is shown that biased user association improves the utility of the heterogeneous networks. A survey about user association for 5G networks is presented in [6], pointing out the interference management as the main issue to solve.

Typically, orthogonal resource allocation or fractional frequency reuse is proposed for managing the interference among tiers [7]. For BSs equipped with multiple antennas, the performance achieved by linear precoding techniques assuming perfect knowledge of the channel state information at the transmitters (CSIT) is analyzed in [8]. The use of precoding techniques is aimed at maximizing the achievable degrees of freedom (DoF) by mitigating the interference. In [9], the use of precoding techniques subject to inter-tier and intercell interference is analyzed assuming imperfect CSIT. Focussing on the achievable DoF, the performance of interference alignment (IA) in heterogeneous networks is analyzed in [10]. In these works, the partial connectivity among tiers is exploited for improving the achievable DoF. Recently, this concept is extended to heterogeneous networks composed of macro and pico cells in [11].

The transmission schemes described above for maximizing the DoF are based on CSIT knowledge. In this work, we focus on the implementation of blind IA (BIA) for users equipped with reconfigurable antennas [12]. Basically, a reconfigurable antenna is able to modify its radiation pattern among a set of possible patterns referred to as preset modes [13], [14]. Each preset mode of a reconfigurable antenna provides a linearly independent channel response regarding all other preset modes. Moreover, in the absence of reconfigurable antennas, an opportunistic BIA is proposed in [15] based on exploiting the coherence time variations as preset modes.

The concept of BIA based on reconfigurable antennas was introduced for the broadcast channel (BC) in [12], which is referred to as sBIA from now on. During the last decade, several works have proposed alternative BIA schemes for different scenarios and applications. For instance, the use of BIA for orthogonal frequency division multiplexing (OFDM) interference channels was recently proposed in [16] and an alternative BIA considering fairness for SNR-limited users is derived in [17]. The performance of BIA applied to cellular networks in comparison with linear precoding schemes and taking into consideration the costs of providing CSIT is analyzed in [18]. In [19], a network BIA (nBIA) scheme

Maximo Morales-Cespedes and Ana Garcia Armada are with the Department of Signal Theory and Communications. Universidad Carlos III de Madrid, Leganés, Spain (maximo@tsc.uc3m.es, agarcia@tsc.uc3m.es).

Luc Vandendorpe is with the Institute of Information and Communication Technologies, Electronics and Applied Mathematics (ICTM). Université Catholique de Louvain, Belgium (luc.vandendorpe@uclouvain.be).

This work has been supported by project IRENE-EARTH (PID2020-115323RB-C33 / AEI / 10.13039/501100011033) and the project GEOVEOLUZ-CM-UC3M.

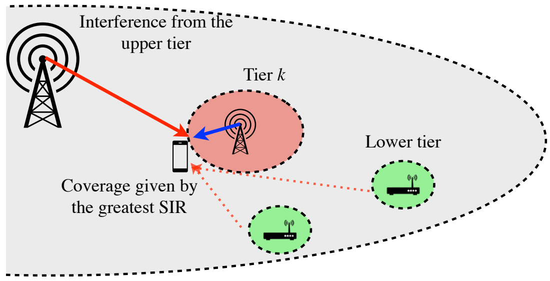


(a) Traditional approach. Each user is connected to the BS that provides the highest SIR. The coverage area in tier $k$ is subject to interference from the upper tiers.

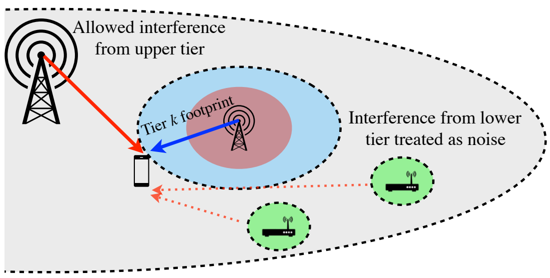


(b) Topological approach. Each user is connected to a tier if the interference from the lower tiers can be treated as noise. The interference from the upper tiers is allowed.

Fig. 1. Traditional and topological approaches for assigning each user to a specific tier.

for cellular networks with partial connectivity is derived. Moreover, it is demonstrated that nBIA achieves the optimal-DoF in symmetric cellular networks. Considering small cell deployments, in [20], a BIA scheme that improves the DoF with respect to the use of BIA independently in each BS is proposed. Still considering small cell deployments, the DoF of two-tier networks without CSIT are derived in [21]. However, these works assume particular characteristics of the small cells, e.g., neglecting the intercell interference among them. The DoF without CSIT for two-tier networks are derived in [22] without focussing on their achievability. Notice that general $K$-tier heterogeneous networks based on BIA transmission have not been considered in prior works to the best of our knowledge.

Focussing on the application of BIA schemes for 5G, the main benefit is to get rid of the closed-loop for CSIT estimation between BSs and users [23]. That is, the pilots for estimating the channel state information at the receiver (CSIR) are transmitted in the same frame as the data without the need for a closed-loop between transmitters and receivers. In [24], avoiding the CSIT is pointed out as a manner of achieving ultra-low latency and lower energy applications.

In this work, we derive a BIA scheme for managing the inter-tier interference in $K$-tier networks without CSIT. The main contributions are:

*1) Interference-allowed tier selection:* Each user is assigned to a tier if and only if the interference from lower tiers can be treated as noise. In contrast, the interference from the upper tiers is allowed around the BS belonging to the selected tier as is shown in Fig. 1(b).

*2) BIA scheme for $K$-tier networks:* Based on the interference-allowed tier selection, a BIA scheme referred to as tier BIA (tBIA) is devised to mitigate the interference in $K$-tier networks. In contrast to previous works, tBIA does not propose a specific BIA transmission scheme but can be applied assuming that each tier employs a BIA scheme selected among most of those available in the state of art.

*3) DoF of $K$-tier networks without CSIT:* The DoF outer-bound for $K$-tier networks in absence of CSIT and cooperation among BSs is derived. To the best of our knowledge, this is the first derivation of the DoF for $K$-tier networks without CSIT.

*4) Optimality of managing the inter-tier interference:* It is demonstrated that transmitting zero-DoF in any tier with the aim of improving the DoF in the lower tiers achieves less DoF in the whole network than managing the inter-tier interference.

Simulation results show that the tBIA provides greater DoF than other BIA schemes that do not manage the inter-tier interference, which are based on a traditional approach for assigning a specific tier to each user. Furthermore, when applied to heterogeneous cellular networks tBIA ensures a constant rate even if the considered users are subject to interference from upper tiers.

The remainder of this paper is organized as follows. In Section II, the system model for $K$-tier networks is presented. In Section III, we describe the structure of BIA schemes to introduce some useful concepts. The tBIA scheme is derived in Section IV. In Section V, the closed-form expressions of the rates achieved by the tBIA scheme are presented. In Section VI, we derive the DoF outer-bound and several subsequent corollaries. Section VII presents some simulation results. Finally, Section VIII provides concluding remarks.

*Notation*. Bold upper case and lower case letters denote matrices and vectors, respectively, $\mathbf{I}_M$ and $\mathbf{0}_M$ denote the $M \times M$ identity and zero matrices, respectively, while $\mathbf{0}_{M,N}$ corresponds to the $M \times N$ zero matrix, $\mathbf{1}_M$ is the $M \times 1$ all ones vector, $\otimes$ represents the Kronecker product, $[\,]^T$ and $[\,]^H$ are the transpose and the hermitic transpose operators, respectively, $\mathbb{E}$ is the statistical expectation, $\mathrm{col}\{\}$ is the column operator that stacks the considered vectors in a single column and $\lceil\ \rceil$ is the ceiling operator that selects the nearest integer towards minus infinity.

## II. System Model

We consider a $K$-tier, $\mathcal{K} = \{1, 2, \dots, K\}$, network where tier $k$ is composed of $B_k$, $\mathcal{B}_k = \{b_{k,1}, \dots, b_{k,B_k}\}$, BSs equipped with $M_k$ antennas each. The total number of antennas in tier $k$ is denoted as $M_{\Sigma_k} = B_k M_k$. The signal transmitted in tier $k$ at time $n$ can be written as

$$\mathbf{x}^{[k]}[n] = \left[\mathbf{x}^{[b_{k,1}]}[n]^T \quad \cdots \quad \mathbf{x}^{[b_{k,B_k}]}[n]^T\right]^T \in \mathbb{C}^{M_{\Sigma_k} \times 1}, \quad (1)$$

where $\mathbf{x}^{[b_{k,j}]}[n] \in \mathbb{C}^{M_k \times 1}$ is the signal transmitted by BS $b_{k,j}$, $j \in \{1, \dots, B_k\}$. Each user knows the radio signal strength[1] from each BS and the tier to which the BS belongs. Thus, the following tier selection and user categorization is carried out.

[1]This information can be usually extracted from the common pilot channel (CPICH) for most of the cellular standards.

TABLE I
LIST OF SYSTEM MODEL AND BIA PARAMETERS

| Variable | Description | Variable | Description |
|---|---|---|---|
| $K$ | Number of tiers in the network | $U_k$ | Number of users in tier $k$ |
| $k$ | $k$-th tier of the network | $U_{p,k}$ | Number of private users in each BS of tier $k$ |
| $k'$ | Upper tiers of tier $k$, $\{1,\dots,k-1\}$ | $U_{sh,k}$ | Number of shared users among BSs of tier $k$ |
| $k*$ | Lower tiers of tier $k$, $\{k+1,\dots,K\}$ | $\Upsilon_{\iota,k}$ | $\iota$-th generic user in tier $k$ |
| $B_k$ | Number of BSs in tier $k$ | $p_{i,b_{j,k}}$ | $i$-th private user in BS $j$ of tier $k$ |
| $b_{j,k}$ | $j$-th BS in tier $k$ | $sh_{i',k}$ | $i'$-th shared user among the BSs of tier $k$ |
| $M_k$ | Number of antennas in each BS of tier $k$ | $\mathbf{x}^{[k]}[n]$ | Signal transmitted by the BSs in tier $k$ |
| $M_{\Sigma_k}$ | Total number of antennas in tier $k$ | $\mathbf{x}^{[b_{k,j}]}[n]$ | Signal transmitted by BS $j$ in tier $k$ |
| $P_k$ | Power transmitted by each BS in tier $k$ | $P_{th}$ | Power threshold |
| $y^{[p_{i,b_{j,k}}]}$ | Signal received by private user $p_{i,b_{j,k}}$ | $y^{[sh_{i',k}]}[n]$ | Signal received by shared user $sh_{i',k}$ |
| $\mathbf{h}^{[p_{i,b_{j,k}}]}(l)$ | Channel between the BSs of tier $k$ and private user $p_{i,b_{j,k}}$ for preset mode $l$ | $\mathbf{h}^{[sh_{i',k}]}(l')$ | Channel between the BSs of tier $k$ and shared user $sh_{i',k}$ for preset mode $l'$ |
| $\mathbf{g}^{[p_{i,b_{j,k}},k']}(l)$ | Channel between upper tier $k'$ and private user $p_{i,b_{j,k}}$ for preset mode $l$ | $\mathbf{g}^{[sh_{i',k}]}(l')$ | Channel between upper tier $k'$ and shared user $sh_{i',k}$ for preset mode $l'$ |
| $z^{[p_{i,b_{j,k}}]}$ | Noise at private user $p_{i,b_{j,k}}$ | $z^{[sh_{i',k}]}$ | Noise at shared user $sh_{i',k}$ |
| **BIA parameters*** | | | |
| $\mathbf{X}_k$ | Signal transmitted during a supersymbol | $\mathbf{W}^{[\Upsilon_{\iota,k}]}$ | Precoding matrix for user $\Upsilon_{\iota,k}$ |
| $N^{[\Upsilon_{\iota,k}]}$ | Number of alignment blocks allocated to user $\Upsilon_{\iota,k}$ | $\ell$ | $\ell$-th alignment block for each user |
| $\mathbf{u}_\ell^{[\Upsilon_{\iota,k}]}$ | Symbol intended to user $\Upsilon_{\iota,k}$ during its $\ell$-th alignment block | $\mathbf{u}_T^{[\Upsilon_{\iota,k}]}$ | Symbols transmitted during the $N^{[\Upsilon_{\iota,k}]}$ alignment blocks of user $\Upsilon_{\iota,k}$ |
| $f^{[\Upsilon_{\iota,k}]}$ | Temporal function that defined the switching pattern of user $\Upsilon_{\iota,k}$ | $\mathbf{f}^{[\Upsilon_{\iota,k}]}$ | Vector with the preset modes selected by user $\Upsilon_{\iota,k}$ during the supersymbol in tier $k$ |
| $\Lambda_k$ | Length of the supersymbol for the BIA scheme in tier $k$ | $\Lambda_{B1,k}$ | Length of the Block 1 for the BIA scheme in tier $k$ |
| $\Lambda_{B2,k}$ | Length of the Block 2 for the BIA scheme in tier $k$ | $\Lambda_{\text{tBIA}}$ | Length of the resulting tBIA supersymbol |
| $\mathbf{f}_{\text{tBIA}}^{[\Upsilon_{\iota,k}]}$ | Vector with the preset modes selected by user $\Upsilon_{\iota,k}$ during the tBIA supersymbol | $\mathbf{W}_{\text{tBIA}}^{[\Upsilon_{\iota,k}]}$ | Resulting precoding matrix for user $\Upsilon_{\iota,k}$ during the tBIA supersymbol |
| $\text{DoF}_k$ | DoF of the BIA scheme in tier $k$ | $\text{DoF}_{\text{tBIA},k}$ | DoF of the tBIA scheme |

* The generic user $\Upsilon_{\iota,k}$ may correspond to a private, shared or any other user categorization.

### A. Path loss and tier selection

The transmitted signals in tier $k$ are subject to an average power constraint $E\left\{\|\mathbf{x}^{[b_{k,j}]}[n]\|^2\right\} \leq P_k$, where $P_1 \geq P_2 \geq \cdots \geq P_K$. Thus, the power received at location $\bar{\mathbf{z}}$ is $P_r(\bar{\mathbf{z}}) = P_k|\bar{\mathbf{z}} - \bar{\mathbf{b}}_{k,j}|^{-\alpha}$, where $\bar{\mathbf{z}}$ and $\bar{\mathbf{b}}_{k,j}$ are the location in Cartesian coordinates of the position of interest and the BS $b_{k,j}$, respectively, and $\alpha$ is the propagation index. For the considered tier selection, each user is connected to tier $k$ if and only if the power received from lower tiers $k^\star > k$, $k^\star \in \{k+1,\dots,K\}$, is below a threshold $P_{\text{th}}$ from which the received power can be treated as noise. Thus, a user at location $\bar{\mathbf{u}}$ is associated to tier $k$ if

$$P_{k^\star}\left(\min|\bar{\mathbf{u}} - \bar{\mathbf{b}}_{k^\star,j}|^{-\alpha}\right) < P_{\text{th}},\ \forall k^\star < k. \tag{2}$$

As a consequence, the users associated to tier $k$ may be subject to interference from the upper tiers $k' < k$, $k' \in \{1,\dots,k-1\}$.

### B. User categorization

After tier selection, the tier $k$ contains $U_k$ generic users $\Upsilon_{\iota,k}$, $\iota = \{1,\dots,U_k\}$. The concept of generic user is proposed to specify that after tier selection a user categorization is carried out. In the following, we consider a user categorization based on private and shared users. However, other user categorization can be considered. The $U_k$ users in tier $k$ can be treated as either *private users*, which receive a strong signal from a single BS of tier $k$, or *shared users* connected to the $B_k$ BSs of tier $k$. Each BS $b_{j,k}$, $j \in \{1,\dots,B_k\}$, sends information to the private users denoted as $\mathcal{U}_{p,k} = \{p_{1,b_{j,k}},\dots,p_{U_p,b_{j,k}}\}$ and to the shared users $\mathcal{U}_{sh,k} = \{sh_{1,k},\dots,sh_{U_{sh},k}\}$, where $U_{p,b_{j,k}}$ and $U_{sh,k}$ are the number of private users for BS $b_{j,k}$ and the number of shared users in the tier $k$, respectively. Thus, the total number of users in tier $k$ is $\sum_{j=1}^{B_k} U_{p,b_{j,k}} + U_{sh,k}$.

The reconfigurable antenna of private user $p_{i,b_{j,k}}$, $i \in \{1,\dots,U_{p,b_{j,k}}\}$, switches among $M_k$ preset modes. Denoting the preset mode selected by the reconfigurable antenna of user $p_{i,b_{j,k}}$ at time $n$ as $l \in \{1,\dots,M_k\}$, the signal received by user $p_{i,b_{j,k}}$ can be written as

$$\begin{aligned} y^{[p_{i,b_{j,k}}]}[n] &= \mathbf{h}^{[p_{i,b_{j,k}}]}\left(l[n]\right)^T \mathbf{x}^{[k]}[n] \\ &\quad + \sum\nolimits_{k'=1}^{k-1} \mathbf{g}^{[p_{i,b_{j,k}},k']}\left(l[n]\right)^T \mathbf{x}^{[k']}[n] + z^{[p_{i,b_{j,k}}]}[n], \end{aligned} \tag{3}$$

where $\mathbf{h}^{[p_{i,b_{j,k}}]}\left(l[n]\right) \in \mathbb{C}^{B_k M_k \times 1}$ denotes the channel vector between the $B_k$ BSs of tier $k$ and user $p_{i,b_{j,k}}$ associated to the channel response for preset mode $l$. The channel vector between BS $b_{j,k}$ and user $p_{i,b_{j,k}}$ for preset mode $l$ selected at time $n$ is denoted as $\bar{\mathbf{h}}^{[p_{i,b_{j,k}}]}(l[n]) \in \mathbb{C}^{M_k \times 1}$. Thus, omitting the preset mode index for ease of representation, the structure of $\mathbf{h}^{[p_{i,b_{j,k}}]}$ for any preset mode is given by

$$\begin{aligned}\mathbf{h}^{[p_{i,b_{j,k}}]} &= \left[\bar{\mathbf{h}}^{[p_{i,b_{1,k}}]^T} \quad \dots \quad \bar{\mathbf{h}}^{[p_{i,b_{j,k}}]^T} \quad \dots \quad \bar{\mathbf{h}}^{[p_{i,b_{B_k,k}}]^T}\right]^T \\ &= \left[\mathbf{0}_{a,1}^T \quad \dots \quad \bar{\mathbf{h}}^{[p_{i,b_{j,k}}]^T} \quad \dots \quad \mathbf{0}_{b,1}^T\right]^T,\end{aligned} \tag{4}$$

where $a = (j-1)M_k$ and $b = (j+1)M_k$. In (3), $\mathbf{g}^{[p_{i,b_{j,k}},k']}(l[n]) \in \mathbb{C}^{M_{k'}\times 1}$ is the channel vector between the $M_{k'}$ antennas of upper tier $k'$, $k' < k$, which transmit the signal $\mathbf{x}^{[k']} \in \mathbb{C}^{M_{k'}\times 1}$, and user $p_{i,b_{j,k}}$. Moreover, $z^{[p_{i,b_{j,k}}]}$ is additive white Gaussian noise (AWGN) with variance $\sigma_z^2$. As can be seen in (4), within tier $k$, the private users only receive a useful signal from BS $b_{j,k}$ while the signals received from any other BSs $b_{j',k}$, $j' \neq j$, are treated as noise.

Similarly, the reconfigurable antenna of each shared user can switch among $M_{\Sigma_k}$ preset modes. The reconfigurable antenna of user $sh_{i',k}$ selects the preset mode $l' \in \{1,\dots,M_{\Sigma_k}\}$ at time $n$. The resulting channel response from the $B_k$ BSs of tier $k$ to user $sh_{i',k}$ for preset mode $l'$ is given by the vector $\mathbf{h}^{[sh_{i',k}]}(l[n]) \in \mathbb{C}^{M_{\Sigma_k}\times 1}$. Thus, the signal received by user $sh_{i',k}$ at time $n$ is

$$\begin{aligned}y^{[sh_{i',k}]}[n] &= \mathbf{h}^{[sh_{i',k}]}(l[n])^T \mathbf{x}^{[k]}[n] \\ &\quad + \sum_{k'=1}^{k-1} \mathbf{g}^{[sh_{i',k},k']}(l[n])^T \mathbf{x}^{[k']}[n] + z^{[sh_{i',k}]}[n],\end{aligned} \tag{5}$$

where, omitting the index of the preset mode selected at time $n$ for ease of representation,

$$\mathbf{h}^{[sh_{i',k}]} = \left[\bar{\mathbf{h}}^{[sh_{i',b_{1,k}}]^T} \quad \dots \quad \bar{\mathbf{h}}^{[sh_{i',b_{B_k,k}}]^T}\right]^T \in \mathbb{C}^{M_{\Sigma_k}\times 1}, \tag{6}$$

and $\bar{\mathbf{h}}^{[sh_{i',b_{j,k}}]} \in \mathbb{C}^{M_k\times 1}$ is the channel between BS $b_{j,k}$ and shared user $sh_{i',k}$. Moreover, $\mathbf{g}^{[sh_{i',k},k']}(l) \in \mathbb{C}^{M_{k'}\times 1}$ is the channel between the transmit antennas of the upper tier $k'$ and the shared user $sh_{i',k}$, $\mathbf{x}^{[k]}[n]$ is as defined in (1) and $z^{[sh_{i',k}]}$ is AWGN with variance $\sigma_z^2$.

The switching patterns of the reconfigurable antenna that determine the preset mode of each user, i.e., the channel response, are predetermined and known beforehand. Moreover, the channels are drawn from a continuous distribution and, therefore, are linearly independent almost surely. The CSIR is known while the transmitters do not have any CSIT. We focus on the temporal dimension without loss of generality, therefore, each symbol extension corresponds to a time slot $n$. Furthermore, the physical channel remains constant across sufficient time slots, and therefore, the channel variations are given by the switching pattern of the users. The system parameters are listed in Table I.

## III. Blind interference alignment for single-tier networks

In this section, we introduce the concept of BIA in order to define some useful notation. This concept is applicable to sBIA, nBIA or other BIA schemes summarized in Table II.

**Definition 1.** *The switching pattern of each user is defined as the series of preset modes that the reconfigurable antenna selects during a specific period of time $\Lambda_k$, where $\Lambda_k$ is the length of the supersymbol in tier $k$. It can be described as a function of time whose values come from the possible channel values that the reconfigurable antenna provides, which is denoted as $f^{[\Upsilon_{\iota,k}]}[n]$ for a generic user. Moreover, we define $\mathbf{f}^{[\Upsilon_{\iota,k}]} \in \mathbb{N}^{\Lambda_k\times 1}$ as the vector that contains the preset modes selected by user $\Upsilon_{\iota,k}$ at each symbol extension of the supersymbol.*

TABLE II

MOST RELEVANT BIA SCHEMES

| Scheme | Applications |
|---|---|
| sBIA [12] | DoF-optimal for broadcast channel. |
| nBIA [19] | DoF-optimal for cellular networks. The users are catergorized in private and shared. |
| cogBIA [21] | DoF-optimal in macro-femto networks neglecting the intercell interference between tiers. |
| semiBIA [20] | BIA scheme for managing the intercell interference small cell networks. The small cells cooperate among them to improve the achievable DoF. |
| shBIA [25] | Diversity in two-BSs cellular networks. The users are catergorized in private and shared. |
| dIC-BIA [26] | Full diversity gain in multiple-input single-output interference channels. |
| UC-BIA [27] | BIA scheme for user-centric schemes where each user is served by distinct number of transmitters. |

**Definition 2.** *The supersymbol is defined as the succession of switching patterns that the users follow during a specific period of time $\Lambda_k$, where $\Lambda_k$ is the length of the supersymbol in tier $k$.*

**Definition 3.** *For BIA schemes, the supersymbol is divided into Block 1 and Block 2 comprising $\Lambda_{\mathrm{B1},k}$ and $\Lambda_{\mathrm{B2},k}$ symbol extensions, respectively, i.e., $\Lambda_k = \Lambda_{\mathrm{B1},k} + \Lambda_{\mathrm{B2},k}$. During Block 1 the symbols intended to the users are transmitted simultaneously while each symbol is transmitted in orthogonal fashion during Block 2.*

**Definition 4.** *An alignment block of user $\Upsilon_{\iota,k}$ is defined as the set of symbol extensions that satisfy the following BIA criterion; the channel of user $\iota$ varies among $M_k$ linearly independent values, where $M_k$ is the number of antennas from which the user receives a useful signal, while the channel state of all other users, $\iota' \neq \iota$ remains constant. The number of alignment blocks of user $\Upsilon_{\iota,k}$ is denoted by $N^{[\Upsilon_{\iota,k}]}$.*

**Definition 5.** *The transmitted signal for any BIA scheme in tier $k$ is given by*

$$\mathbf{X}_k = \sum_{\iota=1}^{U_k} \mathbf{W}^{[\Upsilon_{\iota,k}]} \mathbf{u}_T^{[\Upsilon_{\iota,k}]}, \tag{7}$$

*where $\mathbf{X}^{[k]} = \mathrm{col}\left\{\mathbf{x}^{[k]}[n]\right\}_{n=1}^{\Lambda_k}$, $\mathbf{W}^{[\Upsilon_{\iota,k}]}$ is the precoding matrix for user $\Upsilon_{\iota,k}$ and $\mathbf{u}_T^{[\Upsilon_{\iota,k}]}$ is the vector that contains the symbols transmitted during the supersymbol to user $\Upsilon_{\iota,k}$. The precoding matrices are obtained blindly and they are composed only by $\{0,1\}$ values.*

A generic supersymbol structure is depicted in Fig. 2 highlighting the formation of alignment blocks for each user. For this case, according to Definition 1, the switching pattern of the reconfigurable antenna for user $\Upsilon_{\iota,k}$ in Fig. 2 is given by the temporal function

$$f^{[\Upsilon\iota,k]} = \begin{cases} \mathbf{h}^{[\Upsilon_{\iota,k}]}(1) & \text{for} \quad n \equiv 1, M_k+1\ldots \\ \vdots & \\ \mathbf{h}^{[\Upsilon_{\iota,k}]}(M_k) & \text{for} \quad n \equiv M_k, 2M_k, \ldots \end{cases} \quad (8)$$

where the vector $\mathbf{h}^{[\Upsilon_{\iota,k}]}(l)$ is the channel response for preset mode $l$ of the reconfigurable antenna of user $\Upsilon_{\iota,k}$. That is, for the users in Fig. 2, $\mathbf{f}^{[\Upsilon_{\iota,k}]} = [1, 2, \ldots, M_k, 1, \ldots, M_k, 1\ldots]$ and $\mathbf{f}^{[\Upsilon_{\iota',k}]} = [1, \ldots, 1, 2, \ldots, 2, \ldots]$.

Besides, $N^{[\Upsilon_{\iota,k}]}$, $\ell = \{1, \ldots, N^{[\Upsilon_{\iota,k}]}\}$, alignment blocks are allocated[2] to user $\Upsilon_{\iota,k}$. The symbol transmitted in alignment block $\ell$ of user $\Upsilon_{\iota,k}$ carrying $M_k$ DoF is denoted by $\mathbf{u}_\ell^{[\Upsilon_{\iota,k}]} \in \mathbb{C}^{M_k\times 1}$. The key idea of BIA is to transmit each symbol $\mathbf{u}_\ell^{[\Upsilon_{\iota,k}]}$ during $M_k$ symbol extensions in which the reconfigurable antenna of user $\Upsilon\iota, k$ switches among $M_k$ preset modes. The symbols intended to all other users are transmitted simultaneously during the first $M_k - 1$ symbol extensions of the alignment block, which belong to Block 1. In contrast, the symbol $\mathbf{u}_\ell^{[\Upsilon_{\iota,k}]}$ is transmitted in orthogonal fashion during the last symbol extension of alignment block $\ell$ in Block 2. Let us consider the transmission of $\mathbf{u}_\ell^{[\Upsilon_{\iota,k}]}$ intended to user $\Upsilon_{\iota,k}$ during its $\ell$ alignment block. As can be seen in Fig. 2, the reconfigurable antenna of user $\Upsilon_{\iota,k}$ switches among $1, \ldots, M_k$ preset modes during this alignment block. Therefore, generating $M_k$ linearly independent channel responses, i.e., $\mathbf{h}^{[\Upsilon_{\iota,k}]}(l) \neq \beta\mathbf{h}^{[\Upsilon_{\iota,k}]}(l')+\gamma$, $l \neq l'$, $\forall\beta, \gamma \in \mathbb{R}$. Thus, for user $\Upsilon_{\iota,k}$ who desires the symbol $\mathbf{u}_\ell^{[\Upsilon_{\iota,k}]}$, ignoring momentarily the noise, the signal received during the alignment block $\ell$ is

$$\mathbf{y}^{[\Upsilon_{\iota,k}]} = \underbrace{\begin{bmatrix} \mathbf{h}^{[\Upsilon_{\iota,k}]}(1) \\ \vdots \\ \mathbf{h}^{[\Upsilon_{\iota,k}]}(M_k-1) \\ \mathbf{h}^{[\Upsilon_{\iota,k}]}(M_k) \end{bmatrix}}_{\text{rank}=M_k} \mathbf{u}_\ell^{[\Upsilon_{\iota,k}]} + \underbrace{\begin{bmatrix} \mathbf{h}^{[\Upsilon_{\iota,k}]}(1)\mathbf{u}_\ell^{[\Upsilon_{\iota',k}]} \\ \vdots \\ \mathbf{h}^{[\Upsilon_{\iota,k}]}(M_k-1)\mathbf{u}_{\ell'}^{[\Upsilon_{\iota',k}]} \\ \mathbf{0}_{M_k,1}^T \end{bmatrix}}_{\text{interference}}. \quad (9)$$

Transmission of symbol $\mathbf{u}_\ell^{[\Upsilon_{\iota,k}]}$ generates interference to all other users $\Upsilon_{\iota',k}$, $\iota' \neq \iota$, in Block 1. Since these users maintain a constant preset mode during the transmission of $\mathbf{u}_\ell^{[\Upsilon_{\iota,k}]}$ (see Fig 2), the signal received by users $\Upsilon_{\iota',k}$, $\iota' \neq \iota$ during the transmission of $\mathbf{u}_\ell^{[\Upsilon_{\iota,k}]}$ is

$$\mathbf{y}^{[\Upsilon_{\iota',k}]} = \underbrace{\begin{bmatrix} \mathbf{h}^{[\Upsilon_{\iota',k}]}(1) \\ \vdots \\ \mathbf{h}^{[\Upsilon_{\iota',k}]}(1) \\ \mathbf{h}^{[\Upsilon_{\iota',k}]}(1) \end{bmatrix}}_{\text{rank}=1} \mathbf{u}_\ell^{[\Upsilon_{\iota,k}]} + \underbrace{\begin{bmatrix} \mathbf{h}^{[\Upsilon_{\iota',k}]}(1)\mathbf{u}_\ell^{[\Upsilon_{\iota,k}]} \\ \vdots \\ \mathbf{h}^{[\Upsilon_{\iota',k}]}(M_k-1)\mathbf{u}_{\ell'}^{[\Upsilon_{\iota,k}]} \\ \mathbf{0}_{M_k,1}^T \end{bmatrix}}_{\text{desired symbols for } \Upsilon_{\iota,k}}. \quad (10)$$

[2]The number of alignment blocks per user depends on the BIA scheme. For instance, assuming a BC composed of $M_k$ antennas and $U_k$ users, the sBIA scheme generates $(M_k-1)^{U_k-1}$ alignment blocks per user.

Notice that in (9) the symbol desired for user $\Upsilon_{\iota,k}$ is received through a full rank matrix since it contains the channel responses from $M_k$ preset modes. This condition ensures that the $M_k$ DoF carried by $\mathbf{u}_\ell^{[\Upsilon_{\iota,k}]}$ can be decoded. On the other hand, in (10), it is shown that interference due to transmission of $\mathbf{u}_\ell^{[\Upsilon_{\iota,k}]}$ is aligned in a rank-1 channel matrix, i.e., in a single preset mode, for all other users $\iota' \neq \iota$. Since orthogonal transmission occurs in the last symbol extension of each alignment block, the interference due to transmission of $\mathbf{u}_\ell^{[\Upsilon_{\iota,k}]}$ can be measured by the users $\iota' \neq \iota$ as is shown in Fig. 2. Following this procedure, the interference terms of (9) are cancelled, and therefore, $M_k$ DoF can be decoded free of interference in each alignment block.

## IV. Blind interference alignment for $K$-tier networks

In this section, a BIA scheme for $K$-tier networks referred to as tBIA is presented. The proposed tBIA scheme can be applied assuming that each tier implements any BIA scheme based on alignment blocks composed of Block 1 and Block 2, e.g., [12], [17], [19]. For illustrative purposes, we first describe two specific cases and, after that, we derive the methodology to obtain the supersymbol and the signal transmitted in each tier for the general case.

### *A. Two-tier network. sBIA for $M_1 = 2$, $U_1 = 2$ and nBIA $M_2 = 2$, $B_2 = 2$, $U_{p,b_j,2} = 1$, $U_{sh,2} = 1$.*

We first consider a two-tier network where the sBIA and nBIA schemes are employed in the first and second tiers, respectively. In the first tier a single BS equipped with $M_1 = 2$ antennas transmits to $U_1 = 2$ users. In the second tier, $B_2 = 2$ BSs equipped with $M_2 = 2$ antennas serve to $U_{p,2} = 1$ private user each and $U_{sh,2} = 1$ shared user.

Neglecting the inter-tier interference, the supersymbols that cancel the interference in the first and second tiers are shown in Fig. 3(a) and Fig. 3(b), respectively. The signal transmitted during the 3 symbol extensions that comprise the sBIA supersymbol is

$$\mathbf{X}^{[k]} = \begin{bmatrix} \mathbf{x}^{[k]}[1] \\ \mathbf{x}^{[k]}[2] \\ \mathbf{x}^{[k]}[3] \end{bmatrix} = \underbrace{\begin{bmatrix} \mathbf{I}_2 \\ \mathbf{I}_2 \\ \mathbf{0}_2 \end{bmatrix}}_{\mathbf{W}^{[\Upsilon_{1,k}]}} \mathbf{u}_1^{[\Upsilon_{1,k}]} + \underbrace{\begin{bmatrix} \mathbf{I}_2 \\ \mathbf{0}_2 \\ \mathbf{I}_2 \end{bmatrix}}_{\mathbf{W}^{[\Upsilon_{2,k}]}} \mathbf{u}_1^{[\Upsilon_{2,k}]} \in \mathbb{C}^{2\cdot 3\times 1}, \quad (11)$$

where $\mathbf{u}_1^{[\Upsilon_{\iota,k}]} = [u_{1,1}^{[\Upsilon_{\iota,k}]}, u_{1,2}^{[\Upsilon_{\iota,k}]}]^T \in \mathbb{C}^{2\times 1}$ is the symbol intended to user $\iota$ during the first and single alignment block, and $u_{1,t}^{[\Upsilon_{\iota,k}]}$ is the symbol from antenna $t$, $t = \{1, 2\}$, of the BS. In such a way, the signal transmitted during the 7 symbol

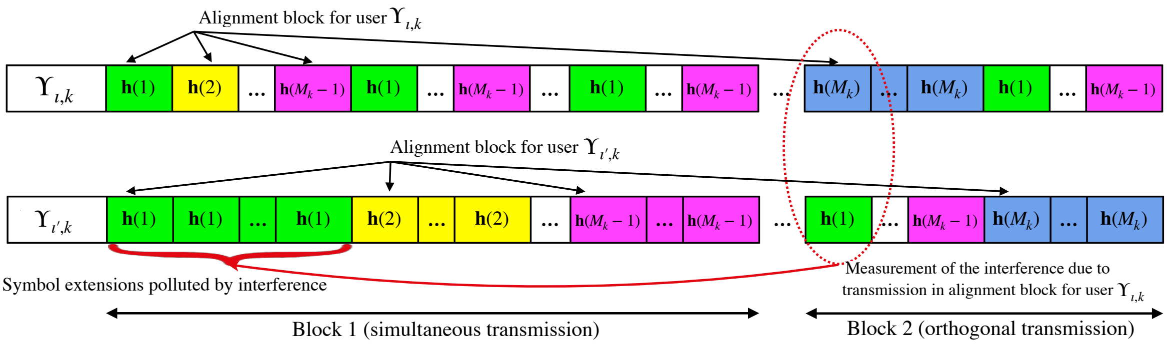


Fig. 2. Interaction between alignment blocks. The user index in the channel vector is omitted, each color represents a preset mode of the considered user.

| | 1 | 2 | 3 |
|---|---|---|---|
| $\Upsilon_{1,k}$ | $\mathbf{h}^{[\Upsilon_{1,k}]}(1)$ | $\mathbf{h}^{[\Upsilon_{1,k}]}(2)$ | $\mathbf{h}^{[\Upsilon_{1,k}]}(1)$ |
| $\Upsilon_{2,k}$ | $\mathbf{h}^{[\Upsilon_{2,k}]}(1)$ | $\mathbf{h}^{[\Upsilon_{2,k}]}(1)$ | $\mathbf{h}^{[\Upsilon_{2,k}]}(2)$ |

(a) Supersymbol of the sBIA scheme for $M_k = 2$ and $U_k = 2$ users.

| | 1 | 2 | 3 | 4 | 5 | 6 | 7 |
|---|---|---|---|---|---|---|---|
| Private users $p_1$ | $\mathbf{h}^{[p_1]}(1)$ | $\mathbf{h}^{[p_1]}(1)$ | $\mathbf{h}^{[p_1]}(1)$ | $\mathbf{h}^{[p_1]}(2)$ | $\mathbf{h}^{[p_1]}(2)$ | $\mathbf{h}^{[p_1]}(2)$ | $\mathbf{h}^{[p_1]}(1)$ |
| Shared user $sh_1$ | $\mathbf{h}^{[sh_1]}(1)$ | $\mathbf{h}^{[sh_1]}(2)$ | $\mathbf{h}^{[sh_1]}(3)$ | $\mathbf{h}^{[sh_1]}(1)$ | $\mathbf{h}^{[sh_1]}(2)$ | $\mathbf{h}^{[sh_1]}(3)$ | $\mathbf{h}^{[sh_1]}(4)$ |

(b) Supersymbol of the nBIA scheme for $B_k = 2$, $M_k = 2$, $U_{p,k} = 1$ private users and $U_{sh,k} = 1$ shared user.

Fig. 3. Supersymbol structures for the proposed setting. Ignoring the inter-tier interference, the first tier implements sBIA while the second tier implements nBIA.

extensions of the nBIA supersymbol is

$$\mathbf{X}^{[k]} = \underbrace{\begin{bmatrix} \mathbf{I}_4 & \mathbf{0} & \mathbf{0} \\ \mathbf{0} & \mathbf{I}_4 & \mathbf{0} \\ \mathbf{0} & \mathbf{0} & \mathbf{I}_4 \\ \mathbf{I}_4 & \mathbf{0} & \mathbf{0} \\ \mathbf{0} & \mathbf{I}_4 & \mathbf{0} \\ \mathbf{0} & \mathbf{0} & \mathbf{I}_4 \\ \mathbf{0} & \mathbf{0} & \mathbf{0} \end{bmatrix}}_{\mathbf{W}^{[p_1]}} \begin{bmatrix} \mathbf{u}_1^{[p_1]} \\ \mathbf{u}_2^{[p_1]} \\ \mathbf{u}_3^{[p_1]} \end{bmatrix} + \underbrace{\begin{bmatrix} \mathbf{I}_4 \\ \mathbf{I}_4 \\ \mathbf{I}_4 \\ \mathbf{0} \\ \mathbf{0} \\ \mathbf{0} \\ \mathbf{I}_4 \end{bmatrix}}_{\mathbf{W}^{[sh_1]}} \mathbf{u}_1^{[sh_1]}, \in \mathbb{C}^{4\cdot 7\times 1}, \tag{12}$$

where $\mathbf{X}^{[k]} = \mathrm{col}\{\mathbf{x}^{[k]}[n]\}_{n=1}^{7}$ is the vector that stacks the signals transmitted during the 7 symbol extensions and $\mathbf{u}_\ell^{[p_i]} = \mathrm{col}\{\mathbf{u}_\ell^{[p_1,j]}\}_{j=1}^{2} \in \mathbb{C}^{4\times 1}$ contains the symbols transmitted to the private users with index $i$ in the alignment block $\ell$, $\ell \in \{1,2,3\}$, where $\mathbf{u}_\ell^{[p_1,j]} \in \mathbb{C}^{2\times 1}$ is the symbol sent by BS $b_{j,k}$ to its private user. Similarly, $\mathbf{u}_1^{[sh_1]} = \mathrm{col}\{\mathbf{u}_1^{[sh_1,j]}\}_{j=1}^{2} \in \mathbb{C}^{4\times 1}$ is the equivalent symbol for user $sh_1$ during a single alignment block where $\mathbf{u}_1^{[sh_1,j]}$ is the symbol sent by BS $b_{j,k}$.

Assuming that the sBIA and nBIA schemes are implemented independently in each tier, the users in second tier are subject to interference from the upper tier. Notice that it is not possible to align the transmission based on nBIA, which comprises 7 symbol extensions, during the 3 symbol extensions of the sBIA supersymbol of the upper tier (see Fig. 3(a) and Fig. 3(b)). This issue can be handled by expanding the supersymbol of first tier until generating a signal space large enough to align the interference in the lower tier. Specifically, the sBIA supersymbol is expanded the length of the nBIA supersymbol, i.e., 7 symbol extensions. The resulting supersymbol comprises $\Lambda_1 \times \Lambda_2 = 21$ symbol extensions. Notice that the resulting supersymbol is composed of Block 1 and Block 2, which comprise the first 7 symbol extensions and the last 14 symbol extensions, respectively. From now on, the resulting supersymbol in tier $k$ for tBIA is divided into super-Block 1 (S-Block$_{1,k}$) where the symbols to the users of that tier are transmitted simultaneously and super-Block 2 (S-Block$_{2,k}$) in which each symbol is transmitted in orthogonal fashion.

The tBIA supersymbol satisfies two conditions. First, the preset mode of the users in first tier remains constant during each alignment block of the users belonging to second tier, which guarantees the alignment between both tiers (see Fig. 4). Secondly, the signal space of first tier is transmitted in orthogonal fashion during S-Block$_{2,1}$. Therefore, the interference from first tier can be measured by the users in second tier if the BSs in that tier remain silent during S-Block$_{2,1}$.

Transmission in second tier, which comprises both S-Block$_{1,2}$ and S-Block$_{2,2}$, occurs during the first 7 symbol extensions. On the other hand, the number of alignment blocks in the first tier is multiplied by 7 because of the considered expansion. The resulting precoding matrices after the expansion can be easily determined using the the right hand of the Kronecker product, i.e., $\mathbf{W}_{\mathrm{tBIA}}^{[\Upsilon_{\iota,1}]} = \mathbf{W}^{[\Upsilon_{\iota,1}]} \otimes \mathbf{I}_{\Lambda_2}$, $\Lambda_2 = 7$. Thus, the signal transmitted in first tier is

$$\mathbf{X}^{[1]} = \sum_{\iota=1}^{2} \mathbf{W}^{[\Upsilon_{\iota,1}]} \mathbf{u}_{\mathrm{T}}^{[\Upsilon_{\iota,1}]} \in \mathbb{C}^{2\cdot 3\cdot 7\times 1}, \tag{13}$$

where $\mathbf{X}^{[1]} = \mathrm{col}\{\mathbf{x}^{[1]}[n]\}_{n=1}^{21}$, $\mathbf{W}^{[\Upsilon_{\iota,1}]} \in \mathbb{C}^{6\times 1}$ is the precoding matrix of user $\Upsilon_{\iota,2}$ in first tier (see (11)), $\mathbf{u}_{\mathrm{T}}^{[\Upsilon_{\iota,1}]} = \mathrm{col}\{\mathbf{u}_\ell^{[\Upsilon_{\iota,1}]}\}_{\ell=1}^{\Lambda_2}$ contains the symbols intended to each user of the first tier where $\mathbf{u}_\ell^{[\Upsilon_{\iota,1}]} \in \mathbb{C}^{2\times 1}$ denotes the symbol allocated to the alignment block $\ell$ of user $\Upsilon_{\iota,1}$.

The expansion in first tier simply multiplies the number of alignment blocks and the supersymbol length by 7. Thus, the DoF in this tier remain the same as before the expansion. Since the sBIA scheme for 2 antennas and 2 users achieve $\frac{4}{3}$ DoF, the

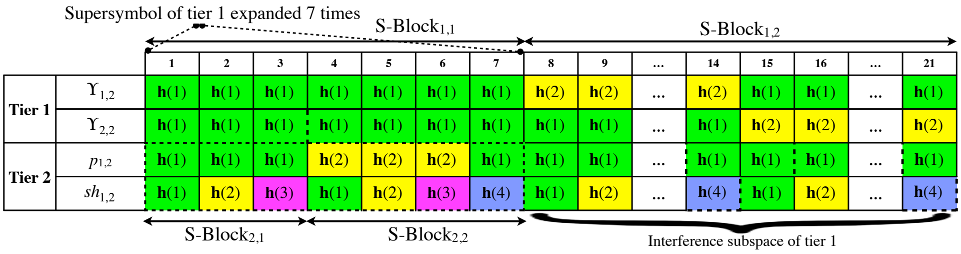


Fig. 4. Supersymbol for tBIA combining sBIA and nBIA in the first and second tiers. The user index is omitted, each color represents a preset mode.

tBIA scheme obtains $\frac{4\times7}{3\times7} = \frac{4}{3}$ DoF in first tier. In the second tier, each private user obtains 3 alignment blocks with 2 DoF each and a single alignment block with 4 DoF is allocated to the shared user. However, instead of 7 symbol extensions, 21 symbol extensions are required in order to cancel the inter-tier interference. As a consequence, $\frac{16}{21}$ DoF are achievable in second tier for the proposed tBIA scheme.

### *B. Three-tier network.* $M_1 = 4$, $M_2 = 3$, $M_3 = 2$, $U_k = 2$

In the following, the tBIA scheme for a 3-tier network is described assuming that each tier contains a single BS equipped with $M_1 = 4$, $M_2 = 3$, $M_3 = 2$ antennas, respectively, serving $U_k = 2$ users each. Besides, it is assumed that each tier implements a sBIA scheme.

First, let us consider only the influence of second tier over the users in third tier while ignoring the first tier. Transmission between both tiers can be aligned by expanding the switching patterns of second tier the length of the supersymbol of third tier, i.e., $\Lambda_3 = 3$ times. Hence, the signal space of the second tier is expanded until it allows the alignment with the third tier. Notice that in Fig. 5 the sBIA supersymbol in third tier can be repeated the length of the Block 1 of second tier, i.e., $\Lambda_{\mathrm{B}1,2} = 4$ times, ensuring the alignment criterion. Besides, the signal space of second tier is transmitted in orthogonal fashion during the last 12 symbol extensions. Thus, the users in third tier can measure the interference subspace because of transmission in second tier if the BS in third tier remains silent during the symbol extensions 13-24.

At this point, both the second and third tiers are subject to interference due to transmission in first tier. Following the BIA criterion, the preset mode of the reconfigurable antenna of each user in first tier must stay constant during the pattern obtained for the lower tiers (see Fig. 5). Therefore, the switching patterns for the users in first tier are expanded the length of the resulting pattern between the second and third tiers, i.e., 24 times, as is shown in Fig. 6. As a consequence, the signal space of first tier is enough to align the inter-tier interference at the lower tiers. As occurs between second and third tier, the pattern obtained in the previous step, i.e., neglecting the first tier, can be repeated $\Lambda_{\mathrm{B}1,1} = 9$ times during the resulting S-Block$_{1,1}$. Thus, the BSs of both second and third tiers remain silent during S-Block$_{2,1}$ in order to measure the inter-tier interference subspace due to transmission in first tier and subtract it afterwards.

The resulting supersymbol comprises 360 symbol extensions. The precoding matrices that determine the transmitted signal in each tier can be obtained as described in (13). According to the structure of the resulting supersymbol, each user in first tier attains 72 alignment blocks providing 4 DoF each. Thus, the DoF per symbol extension of first tier is $\frac{72\times4\times2}{360} = \frac{8}{5}$. Each user in the second and third tiers achieves 54 and 36 alignment blocks with 3 and 2 DoF, respectively. The DoF in second tier are equal to $\frac{54\times3\times2}{360} = \frac{9}{10}$ while in third tier $\frac{36\times2\times2}{360} = \frac{2}{5}$ DoF are achieved.

### *C. General case*

*1) Supersymbol structure for tier $k$:* First, it is necessary to ensure the alignment with the lower tiers. Thus, the preset mode selected by each user in tier $k$ must remain constant while the users of the lower tiers, $k^\star > k$, vary their preset mode in order to generate alignment blocks. To do so, the switching patterns of the users in upper tiers are expanded the needed times to provide a signal space large enough to align the inter-tier interference at lower tiers. This procedure is described in Fig. 7(a). Notice that, the users in tier $K-1$ expand their switching patterns $\Lambda_K$ times, after that, the users in tier $K-2$ expand their switching pattern the lengths of the resulting pattern in tier $K-1$, i.e., $\Lambda_{K-1} \times \Lambda_K$. Following this procedure recursively, the resulting switching pattern for tier $k$ is expanded

$$E_k = \prod_{k^\star=k+1}^{K} \Lambda_{k^\star} \tag{14}$$

times. As a consequence, the switching pattern of the users in first tier is expanded $E_1$ times. The resulting supersymbol provides enough dimensions to align the inter-tier interference to all the users in lower tiers $k > 1$. Therefore, the supersymbol length of tBIA scheme comprises

$$\Lambda_{\mathrm{tBIA}} = \prod_{k=1}^{K} \Lambda_k, \tag{15}$$

symbol extensions.

Focussing on first tier, the resulting supersymbol can be divided into S-Block$_{1,1}$ and S-Block$_{2,1}$ where simultaneous and orthogonal transmission is employed, respectively. The interference subspace because of transmission in tier 1 can be measured by all lower tiers $k > 1$ during S-Block$_{2,1}$. As a consequence, transmission in lower tiers $k > 1$ is limited to S-Block$_{1,1}$, which comprises $E_1\Lambda_{\mathrm{B}1,1}$ symbol extensions. Following this methodology, transmission in tier $k$ occurs within S-Block$_{1,k'}$, $k' < k$. According to the expansion of the switching pattern in each tier, in S-Block$_{1,k'}$ there exist enough dimensions to align the interference due to transmission in

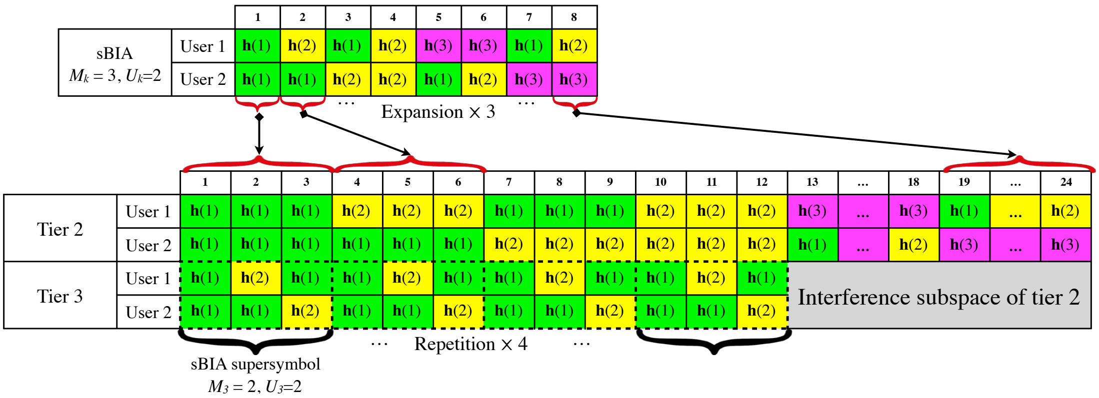


Fig. 5. Patterns of preset modes between third and second tiers of the considered setting. Each color represents a preset mode.

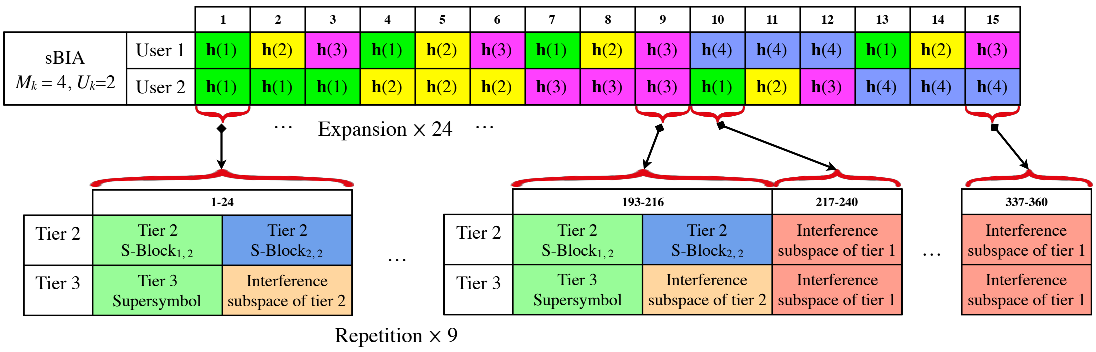


Fig. 6. Supersymbol of the tBIA scheme in a three-tier heterogeneous network for $M_1 = 4$, $M_2 = 3$, $M_3 = 2$, and $U_k = 2$.

upper tiers. Moreover, to ensure that the inter-tier interference can be measured and subtracted, the BSs of tier $k$ remain silent during S-Block$_{2,k'}$. This methodology is depicted in Fig. 8.

The resulting switching patterns after the expansion carried out in second tier can be repeated $\Lambda_{\mathrm{B1,1}}$ times during S-Block$_{1,1}$. Following this procedure, for tier $k$, the resulting switching pattern after the expansion $E_k$ can be repeated

$$R_k = \prod\nolimits_{k'=1}^{k-1} \Lambda_{\mathrm{B1,k'}} \tag{16}$$

times. The switching pattern obtained after the expansion of the BIA-based supersymbol can be repeated $R_k$ times to allow the interference alignment in upper tiers as is shown in Fig. 7.

According to the described procedure, the switching pattern for a generic user is obtained by expanding and repeating the original pattern given by the considered BIA scheme ignoring the inter-tier interference. The repetition and expansion can be managed by the right and left hand of the Kronecker product, respectively, as described above. Specifically, the vector that contains the preset mode selected by user $\Upsilon_{\iota,k}$ during S-Block$_{1,k'}$, $k' < k$, is

$$\mathbf{f}_{\mathrm{tBIA}}^{[\Upsilon_{\iota,k}]}[n] = \mathbf{1}_{R_k} \otimes \mathbf{f}^{[\Upsilon_{\iota,k}]}[n] \otimes \mathbf{1}_{E_k}. \tag{17}$$

*2) Precoding matrices and transmission:* The precoding matrices of the BIA scheme implemented in tier $k$ must be expanded $E_k$ times. After that, the expanded version of the resulting pattern is repeated $R_k$ times. However, notice that the BSs of tier $k$ must remain silent during the transmission of the interference subspace in S-Block$_{2,k'}$, $k' < k$. This issue can be easily handled defining the following repetition matrix

$$\mathbf{C}_k = \left[\mathbf{I}_{\Lambda_{\mathrm{B1},k}}; \quad \mathbf{0}_{\Lambda_{\mathrm{B2},k},\Lambda_{\mathrm{B1},k}}\right]^T, \tag{18}$$

where the zero matrix corresponds to the symbol extensions devoted to measuring the interference because of transmission in upper tiers. Applying the expansion $E_k$ and the repetition $\mathbf{C}_k$ in the right and left hand of the Kronecker product, respectively, the precoding matrix of user $\Upsilon_{\iota,k}$ is

$$\mathbf{W}_{\mathrm{tBIA}}^{[\Upsilon_{\iota,k}]} = \mathbf{C}_1 \otimes \mathbf{C}_2 \otimes \cdots \otimes \mathbf{C}_{k-1} \otimes \mathbf{W}^{[\Upsilon_{\iota,k}]} \otimes \mathbf{I}_{E_k}. \tag{19}$$

Therefore, the signal transmitted in tier $k$ is given by

$$\begin{aligned} \mathbf{X}_k &= \sum_{\iota=1}^{U_k} \mathbf{W}_{\mathrm{tBIA}}^{[\Upsilon_{\iota,k}]} \mathbf{u}_{\mathrm{T}}^{[\Upsilon_{\iota,k}]} \\ &\overset{(a)}{=} \sum_{i=1}^{U_{p,k}} \mathbf{W}_{\mathrm{tBIA}}^{[p_{i},k]} \mathbf{u}_{\mathrm{T}}^{[p_{i,b_{j},k}]} + \sum_{i'=1}^{U_{sh,k}} \mathbf{W}_{\mathrm{tBIA}}^{[sh_{i'},k]} \mathbf{u}_{\mathrm{T}}^{[sh_{i'},k]} \end{aligned} \tag{20}$$

where

$$\mathbf{u}_{\mathrm{T}}^{[\Upsilon_{\iota,k}]} = \mathrm{col}\left\{\mathbf{u}_{\ell}^{[\Upsilon_{\iota,k}]}\right\}_{\ell=1}^{R_k \times N^{[\Upsilon_{\iota,k}]} \times E_k}. \tag{21}$$

Recall that $N^{[\Upsilon_{\iota,k}]}$ denotes the number of alignment blocks of user $\Upsilon_{\iota,k}$ for the BIA scheme in tier $k$. The step (a) considers the user categorization based on private and shared users for

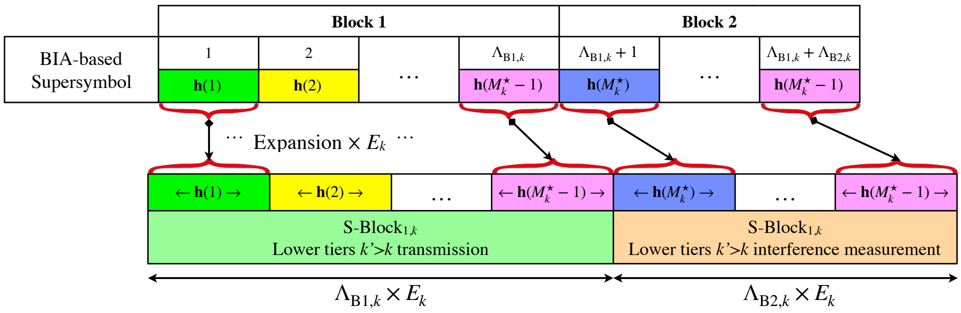


(a) Supersymbol expansion in the tier $k$.

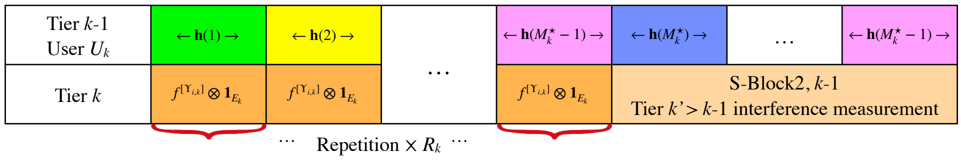


(b) Repetition of the pattern obtained after the expansion described above.

Fig. 7. Construction of the tBIA supersymbol for the tier $k$.

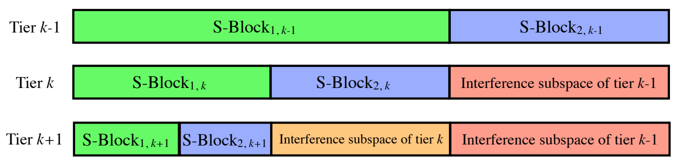


Fig. 8. Structure of S-Block$_{1,k}$, S-Block$_{2,k}$ and the interference subspace for the tier $k$ and subsequent upper and lower tiers.

nBIA. The construction of $\mathbf{u}_T^{[p_{i,k}]}$ and $\mathbf{u}_T^{[sh_{i',k}]}$ follows the same structure as (21) and the precoding matrices $\mathbf{W}_{\text{tBIA}}^{[p_i,k]}$ and $\mathbf{W}_{\text{tBIA}}^{[sh_{i'},k]}$ are given by (19). Other categorization for alternative BIA schemes could be implemented following the procedure described above.

*3) Cancellation of the inter-tier interference:* The last step consists on determining the preset mode selected by each user during the symbol extensions in which the inter-tier interference is measured and subtract it afterwards. The intervals of symbol extensions where the BSs of tier $k$ must remain silent are already defined in (18) and (19).

Consider first the influence of tier $K-1$ in tier $K$. During S-Block$_{2,K-1}$, each user in tier $K$ must select the same preset mode as in the symbol extensions polluted by interference because of transmission in tier $K-1$. This procedure results similar to the interaction between two alignment blocks described in Fig. 2. Because of the expansion carried out in tier $K-1$ (see (14)) the switching pattern obtained in tier $K$ can be repeated $R_K$ times. Thus, the preset mode selected by each user of tier $K$ during the symbol extensions belonging to S-Block$_{2,K-1}$ is given by

$$f_{\text{tBIA}}^{[\Upsilon_\iota,K]}[n'] = f^{[\Upsilon_\iota,K]}\left[n' \mod \Lambda_K \times R_K\right], \tag{22}$$

where $n' \in \{\Lambda_K \times R_K, \ldots, \Lambda_K \times \Lambda_{K-1}\}$. After that, the resulting pattern is repeated $\Lambda_{B1,K-1}$ times because of the extension carried out in tier $K-2$. Following this methodology recursively, the inter-tier interference because of transmission in upper tier $k$ at any user in tier $k^\star$, $k^\star > k$, corresponds to the preset mode

$$f_{\text{tBIA}}^{[\Upsilon_\iota,k^\star]}[n'] = f^{[\Upsilon_\iota,k^\star]}\left[n' \mod E_k \times \Lambda_{B1,k}\right], \tag{23}$$

where $n' \in \{E_k \times \Lambda_{B1,k}+1, \ldots, E_k \times E_k\Lambda_k\}$.

## *D. Achievable Degrees of Freedom*

The proposed tBIA scheme is based on repeating and expanding the switching patterns of the BIA schemes employed in each tier. The expansion and repetition procedures do not involve any penalty in terms of DoF. However, since transmission in tier $k$ occurs strictly in S-Block$_{1,k'}$, $k' < k$, the achievable DoF per symbol extension in tier $k$ is

$$\text{DoF}_{\text{tBIA},k} = \text{DoF}_k \prod_{k'=1}^{k-1} \frac{\Lambda_{B1,k'}}{\Lambda_{k'}}, \tag{24}$$

where $\text{DoF}_k$ denotes the DoF per symbol extension of the BIA scheme considered in tier $k$. Recall that tBIA can be applied considering that each tier implements any BIA scheme based on the structure described in Section III. The most relevant BIA schemes are listed in Table II.

# V. Achievable Rates by Tier Blind Interference Alignment

For tBIA, the closed-form expression of the achievable rate depends on the BIA schemes considered in each tier. In general, the achievable rate of a generic user $\Upsilon_{\iota,k}$ in tier $k$ can be written as

$$R^{[\Upsilon_{\iota,k}]} = \Delta^{[\Upsilon_{\iota,k}]}\mathbb{E}\left[\log\det\left(\mathbf{I} + \bar{P}^{[\Upsilon_{\iota,k}]}\mathbf{A}^{[\Upsilon_{\iota,k}]}\tilde{\mathbf{R}}_z^{[\Upsilon_{\iota,k}]^{-1}}\right)\right], \tag{25}$$

where $\mathbf{A}^{[\Upsilon_{\iota,k}]} = \mathbf{H}^{[\Upsilon_{\iota,k}]}\mathbf{H}^{[\Upsilon_{\iota,k}]^H}$ is given by the channel matrix of the generic user $\Upsilon_{\iota,k}$,

$$\mathbf{H}^{[\Upsilon_{\iota,k}]} = \left[\mathbf{h}^{[\Upsilon_{\iota,k}]}(1)^T \quad \dots \quad \mathbf{h}^{[\Upsilon_{\iota,k}]}(M_k^\star)^T\right]^T \in \mathbb{C}^{M_k^\star \times M_k^\star}, \tag{26}$$

and $M_k^\star$ denotes the number of antennas from which the user receives a useful signal, e.g., $M_k$ and $M_{\Sigma_k}$ for the private and shared users, respectively. In (25), $\Delta^{[\Upsilon_{\iota,k}]}$ is the ratio of number of alignment blocks to the tBIA supersymbol length and $\bar{P}^{[\Upsilon_{\iota,k}]}$ is the power allocated to each alignment block[3]. The covariance matrix of the interference plus noise for user $\Upsilon_{\iota,k}$ is

$$\tilde{\mathbf{R}}_z^{[\Upsilon_{\iota,k}]} = \mathbf{R}_z^{[\Upsilon_{\iota,k}]} + \sum_{k^\star=k+1}^{K} P_{k^\star}\mathbf{H}_{\mathrm{I}_k^\star}^{[\Upsilon_{\iota,k}]}\mathbf{H}_{\mathrm{I}_k^\star}^{[\Upsilon_{\iota,k}]^H}, \tag{27}$$

where $\mathbf{H}_{\mathrm{I}_k^\star}^{[\Upsilon_{\iota,k}]} \in \mathbb{C}^{M_k^\star \times M_k^\star}$ is the channel matrix from the BSs of the lower tiers and the $M_k^\star$ preset modes of the reconfigurable antenna for user $\Upsilon_{\iota,k}$ and $P_{k^\star}$ is the transmission power of the tier $k^\star$. Moreover, $\mathbf{R}_z^{[\Upsilon_{\iota,k}]}$ is the noise enhancement matrix because of the interference subtraction,

$$\mathbf{R}_z^{[\Upsilon_{\iota,k}]} = \begin{bmatrix} \left(\bar{U}_k + \sum_{k'=1}^{k-1} U_{k'}\right)\mathbf{I}_{M_k^\star-1} & \mathbf{0} \\ \mathbf{0} & \sum_{k'=1}^{k-1} U_{k'} \end{bmatrix}, \tag{28}$$

where $\bar{U}_k$ corresponds to the number of users in tier $k$ whose transmission interferes to the symbols intended to user $\Upsilon_{\iota,k}$.

It is worth noticing that the user rate depends on parameters such as the number of alignment blocks per user, the supersymbol length, the structure of the channel matrix and the number of interference terms that are subtracted, which are given by the BIA scheme considered in each tier. Notice that obtaining the optimal DoF does not means maximizing the sum-rate. In general, there does not exist a methodology for maximizing the sum-rate in $K$-tier networks since it depends on the BIA scheme implemented in each tier.

## VI. Degrees of Freedom of $K$-Tier heterogeneous Networks Without CSIT

In this section, we derive the DoF for $K$-tier heterogeneous networks without CSIT. For convenience of representation the following parameter is defined

$$\nu_k = \begin{cases} 1 & \text{if } k = 1 \\ \frac{M_{k-1}}{M_k} & \text{if } 1 < k < K \\ \frac{M_{K-1}}{B_K M_K} & \text{if } k = K, \end{cases} \tag{29}$$

we assume that $\frac{M_{k-1}}{M_k} \in \mathbb{N}$ and $\frac{M_{K-1}}{B_K M_K} \in \mathbb{N}$ for the sake of simplicity. Without loss of generality, let us focus on tier $K$ where $B_K = 2$ BSs serve to $U_{p,b_{j,K}}$, $j \in \{1, 2\}$, private users each while $U_{sh,K}$ shared users are served simultaneously by both BSs. The extension to $B_K$ BSs is straightforward. The messages for the private and shared users in tier $K$ are defined as $\mathcal{W}^{[\mathcal{U}_{p,b_{j,K}}]} = \left\{W^{[p_{1,b_{j,K}}]}, \dots, W^{[p_{U_{p,b_{j,K}}},K]}\right\}$ and $\mathcal{W}^{[\mathcal{U}_{sh,K}]} = \left\{W^{[sh_{1,K}]}, \dots, W^{[sh_{U_{sh,K}},K]}\right\}$, respectively, and $\mathcal{W}^{[k]}$, $k \in \{1, \dots, K\}$, denotes the whole set of messages transmitted in tier $k$. Furthermore, the messages transmitted in tier $K$ generate the rates for the private and the shared users $\mathcal{R}^{[\mathcal{U}_{p,b_{j,K}}]} = \left\{R^{[p_{1,b_{j,K}}]}, \dots, R^{[p_{p_{U_{p,b_{j,K}}}},K]}\right\}$ and $\mathcal{R}^{[\mathcal{U}_{sh,K}]} = \left\{R^{[sh_{1,K}]}, \dots, R^{[sh_{U_{sh,K}},K]}\right\}$, respectively. Moreover, the sum-rate of the users of tier $k$ is denoted as $R_\Sigma^{[k]}$. Similarly, $d_{\Sigma_{p,b_{j,K}}}$ and $d_{\Sigma_{sh,K}}$ denote the sum-DoF of the private users assigned to BS $b_{j,K}$ and the shared users in tier $K$, respectively. The sum-DoF of the users in tier $k$ is denoted by $d_{\Sigma_k}$. Besides, we denote the regular entropy as $H(\cdot)$ and the differential entropy as $h(\cdot)$.

**Theorem 1.** *For a $K$-tier network as described above the achievable DoF in tier $K$ is given by solving the following linear problem*

$$\text{maximize} \quad d_{\Sigma_{sh,K}} + d_{\Sigma_{p,b_{1,K}}} + d_{\Sigma_{p,b_{2,K}}} \tag{30}$$

$$\text{subject to}$$

$$U_{p,b_{2,K}} A_{b_{1,K}} d_{\Sigma_{p,b_{1,K}}} + U_{p,b_{1,K}} A_{b_{2,K}} d_{\Sigma_{p,b_{2,K}}} + U_{p,b_{1,K}} U_{p,b_{2,K}} d_{\Sigma_{sh,K}} \le U_{p,b_{1,K}} U_{p,b_{2,K}} M_{\Sigma_K} C_K \tag{31}$$

$$A_{sh,K} d_{\Sigma_{sh,K}} + U_{sh,K}\left(d_{\Sigma_{p,b_{1,K}}} + d_{\Sigma_{p,b_{2,K}}}\right) \le U_{sh,K} M_{\Sigma_K} C_K. \tag{32}$$

*where $A_{b_{1,K}} = M_K + U_{p,b_{1,K}} - 1$, $A_{b_{2,K}} = M_K + U_{p,b_{2,K}} - 1$, $A_{sh,K} = M_{\Sigma_K} + U_{sh,K} - 1$ and $C_K = 1 - \sum_{k=1}^{K-1} \frac{d_{\Sigma_k}}{M_k}$.*

*Proof.* The proof of this theorem follows a recursive methodology. Starting from tier $K$ the outer bound of the rate of user $p_{1,b_{1,K}}$ is obtained considering the messages transmitted in tier $K$, after that, the messages transmitted in tier $K-1$ are considered and, recursively, the outer bound is obtained once the messages in all the tiers $1, \dots, K$ are considered. Summing up these bounds for all the private users the inequality (31) is obtained. The same procedure can be carried out for the shared users obtaining (32). In the following we describe this methodology in detail.

**Tier $K$.** Focusing on private user $p_{1,b_{1,K}}$ without loss of generality, let us consider $M_K$ random realizations of this user, each corresponding to a different realization of the channel. The signal received by the $l$-th realization of private user $p_{1,b_{1,K}}$ is denoted by $y_l^{[p_{1,b_{1,K}}]}$. Since there is no CSIT, each realization should have probability of error approaching zero to achieve reliable decoding. Moreover, the channel is known at the receiver so that it is not a source of uncertainty. Applying Fano's inequality to codebooks spanning $n$ channel uses

$$\begin{aligned} nR^{[p_{1,b_{1,K}}]} \le{}& I\left(W^{[p_{1,b_{1,K}}]}; \left(y_l^{[p_{1,b_{1,K}}]}\right)^n\right) \\ ={}& h\left(\left(y_l^{[p_{1,b_{1,K}}]}\right)^n\right) - h\left(\left(y_l^{[p_{1,b_{1,K}}]}\right)^n | W^{[p_{1,b_{1,K}}]}\right) \\ \le{}& n\left(\log(P_K) + o\left(\log(P_K)\right)\right) \\ &- h\left(\left(y_l^{[p_{1,b_{1,K}}]}\right)^n | W^{[p_{1,b_{1,K}}]}\right) + o(n). \end{aligned} \tag{33}$$

[3]The use of power allocation schemes is limited because of the lack of CSIT. For BIA schemes, uniform and constant power allocation over each alignment block are typically considered [18].

For the sake of an easy explanation and space limitations, the term $o(\log(P_K))+o(n)$ is omitted from now on. Since this is true for every realization $l \in \{1,\ldots,M_K\}$, after adding up the inequality (33) to all $M_K$ realizations and using $h(A,B) \leq h(A)+h(B)$,

$$nM_K R^{[p_{1,b_{1,K}}]} \leq nM_K \log(P_K) - h\left(\left(y_1^{[p_{1,b_{1,K}}]},\ldots,y_{M_K}^{[p_{1,b_{1,K}}]}\right)^n |W^{[p_{1,b_{1,K}}]}\right). \quad (34)$$

Denoting $\mathbf{y}^{[p_{1,b_{1,K}}]} = \left(y_1^{[p_{1,b_{1,K}}]},\ldots,y_{M_K}^{[p_{1,b_{1,K}}]}\right)^n$ and using $h(A,B|C)=h(A|B,C)+h(B|C)$ the messages $\mathcal{W}_*^{[\mathcal{U}_{p,b_{1,K}}]} = \mathcal{W}^{[\mathcal{U}_{p,b_{1,K}}]} \backslash W^{[p_{1,b_{1,K}}]}$ are considered in (34),

$$\begin{aligned} nM_K R^{[p_{1,b_{1,K}}]} \leq & nM_K \log(P_K) \\ & - h\left(\mathcal{W}_*^{[\mathcal{U}_{p,b_{1,K}}]}, \mathbf{y}^{[p_{1,b_{1,K}}]} |W^{[p_{1,b_{1,K}}]}\right) \\ & + h\left(\mathcal{W}_*^{[\mathcal{U}_{p,b_{1,K}}]} |\mathbf{y}^{[p_{1,b_{1,K}}]}, W^{[p_{1,b_{1,K}}]}\right) \end{aligned} \quad (35)$$

$$\begin{aligned} \overset{\text{(a)}}{\leq} & nM_K \log(P_K) - h\left(\mathcal{W}_*^{[\mathcal{U}_{p,b_{1,K}}]} |W^{[p_{1,b_{1,K}}]}\right) \\ & - h\left(\mathbf{y}^{[p_{1,b_{1,K}}]} |\mathcal{W}^{[\mathcal{U}_{p,b_{1,K}}]}\right) \end{aligned} \quad (36)$$

$$\begin{aligned} \overset{\text{(b)}}{\leq} & nM_K \log(P_K) - \sum_{i=2}^{U_{p,b_{1,K}}} R^{[p_{i,b_{1,K}}]} \\ & - h\left(\mathbf{y}^{[p_{1,b_{1,K}}]} |\mathcal{W}^{[\mathcal{U}_{p,b_{1,K}}]}, \mathcal{W}^{[\mathcal{U}_{p,b_{2,K}}]}\right). \end{aligned} \quad (37)$$

In (35), notice that the $M_K$ realizations in $\mathbf{y}^{[p_{1,b_{1,K}}]}$ contain all the possible channel outputs for the private users in BS $b_{1,K}$. Therefore, it must be possible to decode the set of messages to the private users in $b_{1,K}$, i.e., $h\left(\mathcal{W}_*^{[\mathcal{U}_{p,b_{1,K}}]} |\mathbf{y}^{[p_{1,b_{1,K}}]}, W^{[p_{1,b_{1,K}}]}\right) \leq o(n)$. In other words, it only contains uncertainty due to noise distortion. The step (a) employs the chain rule and given the independence between any pair of messages we use $h\left(\mathcal{W}_*^{[\mathcal{U}_{p,b_{1,K}}]} |W^{[p_{1,b_{1,K}}]}\right) = \sum_{i=2}^{U_{p,b_{1,K}}} R^{[p_{i,b_{1,K}}]}$ in the step (b). Besides, in (37) we use the fact that conditionality does not increase the entropy.

Proceeding similarly for private user $p_{1,b_{2,K}}$ in BS $b_{2,K}$ of tier $K$, we obtain a similar inquality as (37). Thus, adding up both inequalities and using $h(A)+h(B) \geq h(A,B)$,

$$\begin{aligned} nM_K & \left(R^{[p_{1,b_{1,K}}]} + R^{[p_{1,b_{2,K}}]}\right) \leq n2M_K \log(P_K) \\ & - \sum_{i=2}^{U_{p,b_{1,K}}} R^{[p_{i,b_{1,K}}]} - \sum_{i=2}^{U_{p,b_{2,K}}} R^{[p_{i,b_{2,K}}]} \\ & - h\left(\mathbf{y}^{[p_{1,b_{1,K}}]}, \mathbf{y}^{[p_{1,b_{2,K}}]} |\mathcal{W}^{[\mathcal{U}_{p,b_{1,K}}]}, \mathcal{W}^{[\mathcal{U}_{p,b_{2,K}}]}\right) \end{aligned} \quad (38)$$

$$\begin{aligned} \overset{\text{(c)}}{\leq} & n2M_K \log(P_K) - nR_{\Sigma_p *}^{[K]} \\ & - h\left(\mathbf{y}^{[p_{1,b_{1,K}}]}, \mathbf{y}^{[p_{1,b_{2,K}}]} |\mathcal{W}^{[K]}\right). \end{aligned} \quad (39)$$

In step (c), the observations $\mathbf{y}^{[p_{1,b_{1,K}}]}, \mathbf{y}^{[p_{1,b_{2,K}}]}$ provide $M_{\Sigma_K} = 2M_k$ generic linear equations, which can therefore be solved to recover $M_{\Sigma_K}$ outputs. Thus, from the entropy term in (38) it is possible to recover the remaining messages in tier $K$, i.e., $\mathcal{R}^{[\mathcal{U}_{sh},K]}$, within a $n(o\log(P))$ term (omitted for space limitations). Thus, after defining $nR_{\Sigma_p *}^{[K]} = R_{\Sigma}^{[K]} - R^{[p_{1,b_{1,K}}]} - R^{[p_{1,b_{2,K}}]}$, we obtain (39). At this point, notice that the $2M_K$ realizations of (39) are polluted by interference from the upper tiers $k = \{1,\ldots,K-1\}$.

**Tier** $K-1$**.** In this step, we introduce the messages transmitted in tier $K-1$ in order to obtain the costs of canceling this inter-tier interference without CSIT. Consider now that we generate auxiliary copies of the private users $p_{1,b_{1,K}}$ and $p_{1,b_{2,K}}$ who want the same messages and have the same statistics as their corresponding user. Let us denote $\mathbf{y}_m^{[p_{1,b_{j,K}}]} = \left(y_{1,m}^{[p_{1,b_{j,K}}]},\ldots,y_{M_K,m}^{[p_{1,b_{j,K}}]}\right)^n$ as the set of $M_K$ realizations of private user $p_{1,b_{j,K}}$. For simplicity, we relabel the original set of observations $\mathbf{y}^{[p_{1,b_{j,K}}]}$ as the first copy of the considered user, which is denoted by $\mathbf{y}_1^{[p_{1,b_{j,K}}]}$. Specifically, consider $\nu_K$ copies of both private users $p_{1,b_{1,K}}$ and $p_{1,b_{2,K}}$ and proceed as in the previous step until we obtain (39). Note that $\nu_K = 1$ if $2M_K \geq M_{K-1}$, and therefore, no auxiliary copies would be required in this step. Adding up the $\nu_K$ copies, which are similar to (39), and using $h(A,B) \leq h(A)+h(B)$ we obtain (40) In step (d) we use $h(A,B|C) = h(A|B,C)+h(B|C)$ considering the set of messages from the subsequent upper tier $\mathcal{W}^{[K-1]}$. In (41), it is possible to decode the messages to the users in tier $K-1$ from $\mathbf{y}_1^{[p_{1,b_{1,K}}]},\ldots,\mathbf{y}_{\nu_K}^{[p_{1,b_{2,K}}]}$, which contains $M_{K-1}$ outputs, only subject to noise distortion. Using the chain rule and the independence between messages, which provide the sum-rate in upper tier, i.e., $R_{\Sigma}^{[K-1]}$, we obtain (42) Note that the realizations $\mathbf{y}_1^{[p_{1,b_{1,K}}]},\ldots,\mathbf{y}_{\nu_K}^{[p_{1,b_{2,K}}]}$ in the last entropy term of (42) are still polluted by the messages sent by the BSs in the upper tiers $k \leq K-2$ while the messages in lower tiers, i.e., $\mathcal{W}^{[K]}, \mathcal{W}^{[K-1]}$ are known.

The procedure described above for tier $K-1$ can be repeated introducing the messages of tier $K-2$ so that the penalty of canceling the interference in that tier can be determined in terms of $R^{[K-2]}$. Thus, the entropy term similar to the last term in (42) would contain $M_{K-2}$ realizations polluted by interference from upper tiers $1,\ldots,K-3$ since the messages $\mathcal{W}^{[K]}, \mathcal{W}^{[K-1]}, \mathcal{W}^{[K-2]}$ are known. Then, the same procedure can be carried out for the remaining tiers.

**Recursively until Tier 1.** The procedure described above can be carried out recursively until the first tier of the considered $K$-tier network. The key idea is based on creating auxiliary copies of the private users until we obtain enough outputs to consider the set of messages sent in the following upper tier and determine the costs in rate by using the chain rule as in (34)-(35). By creating $\nu_k$, $k \in \{1,\ldots,K-1\}$, auxiliary copies with $M_K$ realizations each and following the procedure described above recursively until the first tier we obtain (43)

Replacing $p_{1,b_{1,K}}$ and $p_{1,b_{2,K}}$ with any private user in tier $K$ $p_{i,b_{1,K}}$, $i \in \{1,\ldots,U_{p,b_{1,k}}\}$, and $p_{\breve{i},b_{2,K}}$, $\breve{i} \in \{1,\ldots,U_{p,b_{2,k}}\}$, respectively, after dividing by $n\log(P_K)$, taking first the limit

$$
\begin{aligned}
n\nu_K M_K \left(R^{[p_{1,b_{1,K}}]} + R^{[p_{1,b_{2,K}}]}\right) &\leq n2\nu_K M_K \left(\log(P_K)\right) - n\nu_K R^{[K]}_{\Sigma_p *} \\
&- h\left(\mathbf{y}_1^{[p_{1,b_{1,K}}]}, \mathbf{y}_1^{[p_{1,b_{2,K}}]}, \ldots, \mathbf{y}_{\nu_K}^{[p_{1,b_{1,K}}]}, \mathbf{y}_{\nu_K}^{[p_{1,b_{2,K}}]}, |\mathcal{W}^{[K]}\right) \qquad (40)\\
&\overset{\text{(d)}}{\leq} n2\nu_K M_K \left(\log(P_K)\right) - n\nu_K R^{[K]}_{\Sigma_p *} - h\left(\mathcal{W}^{[K-1]}, \mathbf{y}_1^{[p_{1,b_{1,K}}]}, \mathbf{y}_1^{[p_{1,b_{2,K}}]}, \ldots, \mathbf{y}_{\nu_K}^{[p_{1,b_{1,K}}]}, \mathbf{y}_{\nu_K}^{[p_{1,b_{2,K}}]} |\mathcal{W}^{[K]}\right) \\
&+ \underbrace{h\left(\mathcal{W}^{[K-1]} | \mathbf{y}_1^{[p_{1,b_{1,K}}]}, \mathbf{y}_1^{[p_{1,b_{2,K}}]}, \ldots, \mathbf{y}_{\nu_K}^{[p_{1,b_{1,K}}]}, \mathbf{y}_{\nu_K}^{[p_{1,b_{2,K}}]}, \mathcal{W}^{[K]}\right)}_{\leq o(n)} \qquad (41)
\end{aligned}
$$

$$
\begin{aligned}
n\nu_K M_K \left(R^{[p_{1,b_{1,K}}]} + R^{[p_{1,b_{2,K}}]}\right) &\overset{\text{(e)}}{\leq} n2\nu_K M_K \left(\log(P_K)\right) - n\nu_K R^{[K]}_{\Sigma_p *} - nR^{[K-1]}_{\Sigma} \qquad (42)\\
&- h\left(\mathbf{y}_1^{[p_{1,b_{1,K}}]}, \mathbf{y}_1^{[p_{1,b_{2,K}}]}, \ldots, \mathbf{y}_{\nu_K}^{[p_{1,b_{1,K}}]}, \mathbf{y}_{\nu_K}^{[p_{1,b_{2,K}}]}, |\mathcal{W}^{[K]}, \mathcal{W}^{[K-1]}\right)
\end{aligned}
$$

$$
\begin{aligned}
nM_K \prod_{\kappa=1}^{K} \nu_\kappa \left(R^{[p_{1,b_{1,K}}]} + R^{[p_{1,b_{2,K}}]}\right) &\leq n2 \prod_{\kappa=1}^{K} \nu_\kappa M_K \left(\log(P_K)\right) - n \prod_{\kappa=1}^{K} \nu_\kappa R^{[K]}_{\Sigma_p *} - n \sum_{k=1}^{K-1} \prod_{\kappa=1}^{k} \nu_\kappa R^{[k]}_{\Sigma} \\
&- \underbrace{h\left(\mathbf{y}_1^{[p_{1,b_{1,K}}]}, \mathbf{y}_1^{[p_{1,b_{2,K}}]}, \ldots, \mathbf{y}_{\prod_{\kappa=1}^{K}\nu_\kappa}^{[p_{1,b_{1,K}}]}, \mathbf{y}_{\prod_{\kappa=1}^{K}\nu_\kappa}^{[p_{1,b_{2,K}}]}, |\mathcal{W}^{[K]}, \mathcal{W}^{[K-1]}, \ldots, \mathcal{W}^{[1]}\right)}_{\leq o(n)} \qquad (43)
\end{aligned}
$$

$n \to \infty$ and then the limit $P \to \infty$, a rearranging of the terms yields the following DoF outer-bound

$$
\begin{aligned}
(M_K - 1)\left(d^{[p_{i,b_{1,K}}]} + d^{[p_{\tilde{i},b_{2,K}}]}\right) &\leq 2\, M_K \\
&- d_{\Sigma_K} - \sum_{k=1}^{K-1} \frac{d_{\Sigma_k}}{\prod_{\kappa=k+1}^{K} \nu_\kappa}. \qquad (44)
\end{aligned}
$$

This bound holds for the $U_{p,b_{1,K}}$ and $U_{p,b_{2,K}}$ private users in BSs $b_{1,K}$ and $b_{2,K}$, respectively. Adding up the $U_{p,b_{1,K}}$ and $U_{p,b_{2,K}}$ inequalities and after some re-arrangement the inequality (31) in Theorem 1 is obtained.

Consider now the shared user $sh_{1,K}$ of tier $K$ without loss of generality, who wants the messages $W^{[sh_1,K]}$. Similarly to the steps described above for private users, consider $M_{\Sigma_K}$ realizations of the channel for this user. The signal received by the realization $l$ of shared user $sh_{1,K}$ is denoted as $y_l^{[sh_{1,K}]}$. For any realization $l$, applying the Fano's inequality

$$
\begin{aligned}
nR^{[sh_1,K]} &\leq I\left(W^{[sh_1,K]}; \left(y_l^{[sh_1,K]}\right)^n\right) \\
&\leq n\left(\log(P_K) + o\left(\log(P_K)\right)\right) \\
&- h\left(\left(y_l^{[sh_1,K]}\right)^n |W^{[sh_1,K]}\right) + o(n). \qquad (45)
\end{aligned}
$$

Adding up the bound (45) for all $M_{\Sigma_K}$ realizations and following a similar procedure as in the steps (34)-(39) we obtain

$$
\begin{aligned}
nM_{\Sigma_K} R^{[sh_1,K]} &\leq nM_{\Sigma_K} \log\left(P_K\right) - nR^{[K]}_{\Sigma^*_{sh}} \\
&- h\left(\underbrace{\left(y_1^{[sh_1,K]}, \ldots, y_{M_{\Sigma_K}}^{[sh_1,K]}\right)^n}_{2M_K \text{ realizations}} |\mathcal{W}^{[K]}\right), \qquad (46)
\end{aligned}
$$

where $R^{[K]}_{\Sigma^*_{sh}} = R^{[K]}_{\Sigma} - R^{[sh_1,K]}$ and term $o\left(\log(P_K)\right) + o(n)$ is omitted. At this point, we create $\nu_K$ copies of shared user $sh_1$ in tier $K$ who also wants the message $W^{[sh_1,K]}$ and have the same statistics. Thus, we consider the set of messages $\mathcal{W}^{[k]}$ transmitted in the upper tiers, $k \in \{1, \ldots, K-1\}$, to determine the costs in rate because of decoding the desired message free of interference. Recursively until the first tier we obtain the following inequality

$$
\begin{aligned}
nM_{\Sigma_K} \prod_{\kappa=1}^{K} \nu_\kappa R^{[sh_1,K]} &\leq nM_{\Sigma_K} \prod_{\kappa=1}^{K} \nu_\kappa \log\left(P_K\right) \\
&- n \prod_{\kappa=1}^{K} \nu_\kappa R^{[K]}_{\Sigma^*_{sh}} - n \sum_{k=1}^{K-1} \prod_{\kappa=1}^{k} \nu_\kappa R^{[k]}_{\Sigma}. \qquad (47)
\end{aligned}
$$

Replacing the shared user $sh_{1,K}$ with any shared user in tier $K$, $sh_{i',K}$, after dividing by $n\log(P_K)$, taking first the limit $n \to \infty$ and then the limit $P \to \infty$, a rearranging of the terms yields the following DoF outer-bound

$$
(M_{\Sigma_K} - 1)\, d^{[sh_i,K]} \leq M_{\Sigma_K} - d_{\Sigma_K} - \sum_{k=1}^{K-1} \frac{d_{\Sigma_k}}{\prod_{\kappa=k+1}^{K} \nu_\kappa}. \qquad (48)
$$

Since there are $U_{sh,K}$ inequalities as (48), summing the inequalities of all shared users in tier $K$ the bound (32) in Theorem 1 is obtained. $\square$

**Remark 1.** *The DoF for $K$-tier networks without CSIT can be easily extended to the case where $\frac{M_{k-1}}{M_k} \in \mathbb{Z}^+$ by creating enough auxiliary copies of the user of interest to obtain the least common multiple between $M_k$ and $M_{k-1}$. The DoF outer-bound results equal to (31) and (32) considering $\lceil \nu_k \rceil$ copies at tier $k$.*

**Corollary 1.** *For a symmetric network where $U_{p,b_{j,K}} = U_{p,K}$, $j = \{1, \dots, B_K\}$, and $d_{\Sigma_{p,K}}$ denotes the sum-DoF achieved by the private users in each BS in tier $K$, the sum-DoF per symbol extension for the private users of each BS and shared users in tier $K$ are*

$$d_{\Sigma_{p,K}} \leq \frac{M_K U_{p,K}}{\left[(M_K - 1) + U_{sh,K}\frac{(M_K-1)}{(M_{\Sigma_K}-1)} + U_{p,K}\right]} C_K \quad (49)$$

$$d_{\Sigma_{sh,K}} \leq \frac{M_{\Sigma_K} U_{sh,K}}{\left[(M_{\Sigma_K} - 1) + U_{sh,K} + U_{p,K}\frac{(M_{\Sigma_K}-1)}{(M_K-1)}\right]} C_K, \quad (50)$$

*respectively, where $C_K = 1 - \sum_{k=1}^{K-1} \frac{d_{\Sigma_k}}{M_k}$. The DoF for symmetric networks is achieved using nBIA. However, asymmetries typically involves a penalty in DoF as analyzed in detail in [19].*

*Proof.* After some rearrangement of the outer-bound for the generic case (see (31) and (32)) and noting that $M_k = 2M_K \prod_{j=k+1}^{K} \nu_j$ because of definition (29), the sum-DoF outer-bound is given by the following optimization problem

$$\begin{aligned} &\text{maximize } d_{\Sigma_{sh,K}} + d_{\Sigma_{p,K}} && (51)\\ &\text{subject to} \\ &2A_{p,K} d_{\Sigma_{p,K}} + U_{p,K} d_{\Sigma_{sh,K}} \leq 2M_K U_{p,K} C_K && (52)\\ &2\,U_{sh,K} d_{\Sigma_{p;K}} + A_{sh,K} d_{\Sigma_{sh,K}} \leq M_{\Sigma_K} U_{sh,K} C_K && (53)\end{aligned}$$

where $A_{p,K} = (M_K + U_{p,K} - 1)$ and recall that $A_{sh,K} = M_{\Sigma_K} + U_{sh,K} - 1$. The formulated problem can be solved obtaining the inequalities (49) and (50). $\square$

**Corollary 2.** *Assuming that each tier achieves the optimal DoF from the first tier to the following lower tiers, the DoF outer-bound in each BS $j$ of tier $k$ in a symmetric network is*

$$d_{j,k} \leq \frac{M_k \left(U_{p,k} + U_{sh,k}\frac{M_k-1}{M_{\Sigma_k}-1}\right)\prod_{k'=1}^{k-1}(M_{k'} - 1)}{\prod_{\hat{k}=1}^{k} M_{\hat{k}} + \left(U_{p,\hat{k}} + U_{sh,\hat{k}}\frac{M_{\hat{k}}-1}{M_{\Sigma_{\hat{k}}}-1}\right) - 1}. \quad (54)$$

*Proof.* The achievable sum-DoF for the transmitter $j$ of the tier $k$ can be easilty determined as $d_{j,k} \leq d_{\Sigma_{p,k}} + \frac{d_{\Sigma_{sh,k}}}{B_k}$, where $d_{\Sigma_{p,k}}$ and $d_{\Sigma_{sh,k}}$ are given by (49) and (50), respectively. Considering a single tier network, i.e., $K = 1$, the outer-bound for $d_{j,1}$ is obtained when $C_1$ equals 1. Then, considering a second tier and assuming that the first tier reaches the optimal DoF, the penalty of removing the interference subspace because of transmission in first tier at the users in second tier is given by $C_2$, which only depends on the following upper tier $k = 1$. Thus, the DoF in each BS in second tier can be easily determined by (49) and (50). Following this procedure recursively until the $k$-th tier, the bound (54) is obtained. $\square$

**Corollary 3.** *For $K$-tier networks without CSIT that satisfy $B_1 M_1 \geq B_2 M_2 \geq \cdots \geq B_K M_K$, managing the inter-tier interference in tier $K$ provides larger sum-DoF in the whole system than the achievable by tier $K$ when it is considered as an isolated tier. That is, more DoF are achieved by managing the inter-tier interference than switching off the tiers $1, \dots, K-1$ so that the DoF in tier $K$ are maximized.*

*Proof.* The sum-DoF in tier $k$ can be written as $B_k d_{j,k}$, where $d_{j,k}$ is the DoF because of the contribution of each BS in tier $k$ given by (54). Since the DoF in tier $k$ is a non-decreasing function regarding the number of users, the maximum sum-DoF is achieved when the number of users tends to infinity. For the sake of an easy explanation, the following variable is defined $\tilde{U}_k = U_{p,k} + U_{sh,k}\left(\frac{M_k-1}{M_{\Sigma_k}-1}\right)$. Applying this definition in (54) for tier $K$, the sum-DoF assuming that all the upper tiers do not transmit, and therefore, do not interfere in the users of tier $K$, is

$$\lim_{\tilde{U}_K \to \infty} B_K \frac{M_K \tilde{U}_K}{M_K + \tilde{U}_K - 1} = B_K M_K. \quad (55)$$

Independently of the number of users in upper tiers, managing the inter-tier interference in tier $K$ must achieve more DoF than the maximum DoF achievable in tier $K$ assuming that all upper tiers do no interfere, which is given by (55). Thus, the following hypothesis can be formulated,

$$\lim_{\tilde{U}_K \to \infty} \sum_{k=1}^{K} B_k \frac{M_k \tilde{U}_k \prod_{k'=1}^{k-1}(M_{k'} - 1)}{\prod_{\hat{k}=1}^{k}(M_{\hat{k}} + \tilde{U}_{\hat{k}} - 1)} \geq B_K M_K, \quad (56)$$

where the left hand of the inequality corresponds to the sum-DoF in the $K$-tier network assuming that the DoF in tier $K$ are also maximized since the number of users $\tilde{U}_K$ also tends to infinity and the right-hand is given by (55). Thus, the hypothesis (56) can be demonstrated by induction. The base case is determined for a 2-tier network,

$$\begin{aligned}&\lim_{\tilde{U}_2 \to \infty} B_1 \tfrac{M_1 \tilde{U}_1}{M_1 + \tilde{U}_1 - 1} + B_2 \tfrac{M_2 \tilde{U}_2 (M_1-1)}{(M_1+\tilde{U}_1-1)(M_2+\tilde{U}_2-1)} \\ &\qquad = \frac{B_2 M_2 \left(M_1 + \frac{B_1 M_1}{B_2 M_2}\tilde{U}_1 - 1\right)}{(M_1 + \tilde{U}_1 - 1)} \geq B_2 M_2, \quad (57)\end{aligned}$$

where (57) uses the fact that $B_1 M_1 \geq B_2 M_2$. It can be seen that the hypothesis is true for $K = 2$. Thus, by induction the hypothesis (56) must be also true for the $K + 1$ case. Let $\check{k} \in \mathbb{N}^+$ be given and suppose that (56) is true for $\check{k} = k$. We

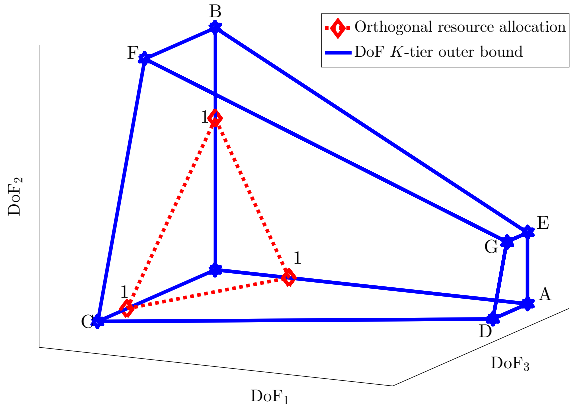


Fig. 9. DoF-region for a three-tier network.

have

$$\lim_{\tilde{U}_{K+1}\to\infty} \sum_{\breve{k}=1}^{K+1} B_{\breve{k}} \frac{M_{\breve{k}}\tilde{U}_{\breve{k}} \prod_{k'=1}^{\breve{k}-1} M_{k'} - 1}{\prod_{\hat{k}=1}^{\breve{k}} M_{\hat{k}} + \tilde{U}_{\hat{k}} - 1} \tag{58}$$

$$\overset{(a)}{\geq} B_K M_K + \frac{B_{K+1}M_{K+1}\prod_{k'=1}^{K} M_{k'} - 1}{\prod_{\hat{k}=1}^{K} M_{\hat{k}} + \tilde{U}_{\hat{k}} - 1} \tag{59}$$

$$= B_{K+1}M_{K+1} \times \frac{\frac{B_K M_K}{B_{K+1}M_{K+1}} \prod_{\hat{k}=1}^{K} M_{\hat{k}} + \tilde{U}_{\hat{k}} - 1 + \prod_{k'=1}^{K} M_{k'} - 1}{\prod_{\hat{k}=1}^{K} M_{\hat{k}} + \tilde{U}_{\hat{k}} - 1} \tag{60}$$

$$\overset{(b)}{\geq} B_{K+1}M_{K+1}\left[1 + \frac{\prod_{k'=1}^{K} M_{k'} - 1}{\prod_{\hat{k}=1}^{K} M_{\hat{k}} + \tilde{U}_{\hat{k}} - 1}\right]. \tag{61}$$

$$\geq B_{K+1}M_{K+1}. \tag{62}$$

The step (a) is given by the induction hypothesis defined in (56) by adding an additional tier $K+1$. Similarly to the 2-tier case analyzed in (57), the step (b) uses the fact that $\frac{B_K M_K}{B_{K+1}M_{K+1}} \geq 1$ and (62) holds because the value in brackets in (61) is always greater than 1. By the principle of induction, it follows that (56) holds for all $K \in \mathbb{N}^+$ and $B_1M_1 \geq B_2M_2 \geq \cdots \geq B_KM_K$. □

## VII. Numerical Results

The DoF region of a three-tier network is depicted in Fig. 9. First, note that the points A, B and C correspond to the optimal DoF neglecting the influence of all other tiers. For a two-tier network, the plane A-B-E corresponds to the DoF region of the first and second tiers ignoring the third tier. Similarly, the planes formed by the points A-C-D and B-C-F correspond to the two-tier network defined by the first and third tiers, and the second and third tiers, respectively, ignoring the remaining tier. For a three-tier network the DoF region is given by the polyhedron shown in Fig. 9. The point G corresponds to the sum-DoF given by (54). Comparing with the DoF region obtained by using orthogonal transmission among tiers, it can be seen the overwhelming benefits of managing the inter-tier interference in $K$-tier networks even when CSIT is not available.

The sum-DoF in a $K = \{2, 3, 4\}$-tier network is analyzed in Fig. 10 and Fig. 11 for $10^2$ and $10^4$ users, respectively, as the density of BSs increases. The users and the BSs are randomly distributed over a $1000 \times 1000\,\mathrm{m}^2$ scenario, after that, tier selection and user categorization is carried out and, finally, the sum-DoF achieved using tBIA is calculated assuming that each tier implements the sBIA/nBIA schemes. Moreover, the sum-DoF achieved by sBIA/nBIA without managing the inter-tier interference is calculated for comparison purposes.

For $10^2$ users, it can be seen in Fig. 10 that tBIA outperforms the use of BIA schemes without managing the inter-tier interference. Indeed, the sum-DoF begins to decrease for high values of density of BSs if the inter-tier interference is not managed. Besides, adding a fourth tier barely increases the sum-DoF. Similarly, for tBIA, the sum-DoF barely increases beyond a number of BSs. That is, for $10^2$ users, deploying more BSs or adding more than 3 tiers is not effective for increasing the network sum-DoF without CSIT. In Table III, the DoF achieved by each tier are detailed (the DoF in tier 4 are omitted because of space limitations). First, notice that the network is overloaded for a single tier since 5.7 DoF are achieved, i.e., 0.057 DoF per user. Adding more tiers distributes the users among several BSs with different transmission power while the BS in tier 1 can be considered as an umbrella tier. Thus, tBIA achieves more DoF in lower tiers since the interference from upper tiers is canceled. For a larger propagation index the usage of the BSs in the lower tiers increases, which provides greater sum-DoF.

In Fig. 11 and Table IV an overloaded network with $10^4$ users, which may correspond to a 5G networks according to [23], is considered. It is worth noticing that if two or more BSs are colocated close to each other and transmitting in the same frequency and time the nBIA scheme considers the users around these BSs as shared users. In this case, it can be seen that the 2-tier network is still overloaded and indeed considering the 4-tier network increases the sum-DoF considerably in comparison with the 3-tier network for tBIA. As also occurs for $10^2$ users, the proposed tBIA scheme outperforms the use of sBIA/nBIA schemes without managing the inter-tier interference. Furthermore, the usage of the lower tiers is improved for a greater propagation index, which results in an improvement of the sum-DoF in the entire network.

In Fig. 12, we analyze the achievable user-rate for a 3-tier network composed of macro, micro and femto cells, i.e., tiers 1, 2, and 3, respectively, where $P_1 = 42$ dBm, $P_2 = 30$ dBm, $P_3 = 21$ dBm. The noise power is $-102$ dBm. The BSs of macro, micro and femto cells are equipped with $M_1 = 6$, $M_2 = 4$ and $M_3 = 2$ antennas, respectively. For ease of representation, we consider a one-dimensional scenario where a single macrocell BS is located at the position 0 serving $U_1 = 12$ users, a single microcell BS is located 315 m away from the macrocell with the aim of improving the rate of $U_2 = 6$ users and 10 femtocells randomly deployed serving $U_3 = 3$ users each. The propagation losses for the macro user is given by the COST231 model and a log-normal model is used for the micro and femto users as described in [21]. Moreover, constant power allocation is assumed [18].

The user-rate in each position of the scenario when it is

TABLE III
DoF AND PERCENTAGE OF THE TOTAL SUM-DoF ACHIEVED IN EACH TIER. 50 BSs IN TIER 2. $10^2$ USERS.

| | | $\alpha = 2$ | | | $\alpha = 3$ | | |
|---|---|---|---|---|---|---|---|
| Tiers | Scheme | Tier 1 | Tier 2 | Tier 3 | Tier 1 | Tier 2 | Tier 3 |
| $K = 1$ | s/n-BIA | 5.7 (100%) | – | – | 5.7 (100%) | – | – |
| $K = 2$ | tBIA | 3.88 (7.4%) | 48.8 (92.6%) | – | 2.9 (4.2%) | 63.3 (95.8%) | – |
| | s/n-BIA | 3.88 (10.8%) | 32.2 (89.2%) | – | 2.9 (5.6%) | 49.4 (94.4%) | – |
| $K = 3$ | tBIA | 4.65 (7.1%) | 47.5 (72.7%) | 13.2 (20.2%) | 3.11 (4.1%) | 42.8 (56.7%) | 29.5 (39.2%) |
| | s/n-BIA | 4.65 (12.5%) | 28.7 (77.2%) | 3.85 (10.3%) | 3.11 (5.6%) | 38.7 (70.1%) | 13.4 (24.3%) |

TABLE IV
DoF AND PERCENTAGE OF THE TOTAL SUM-DoF ACHIEVED IN EACH TIER. 80 BSs IN TIER 2. $10^4$ USERS.

| | | $\alpha = 2$ | | | $\alpha = 3$ | | |
|---|---|---|---|---|---|---|---|
| Tiers | Scheme | Tier 1 | Tier 2 | Tier 3 | Tier 1 | Tier 2 | Tier 3 |
| $K = 1$ | s/n-BIA | $\approx 6$ (100%) | – | – | $\approx 6$ (100%) | – | – |
| $K = 2$ | tBIA | 5.94 (2.4%) | 309 (97.6%) | – | 5.91 (1.9%) | 309 (98.1%) | – |
| | s/n-BIA | 5.94 (4.2%) | 137 (95.8%) | – | 5.91 (2.4%) | 239 (97.6%) | – |
| $K = 3$ | tBIA | 5.97 (1.6%) | 273 (71.3%) | 104 (27.1%) | 5.91 (0.9%) | 302 (47.8%) | 325 (51.3%) |
| | s/n-BIA | 5.97 (2.4%) | 198 (80.4%) | 42.4 (17.2%) | 5.91 (1.2%) | 269 (53.3%) | 230 (45.5%) |

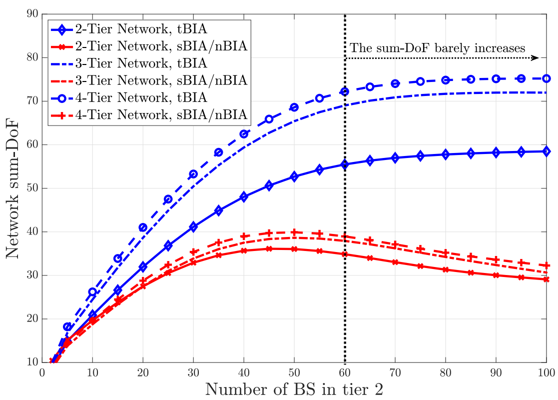


(a) Propagation index $\alpha = 2$.

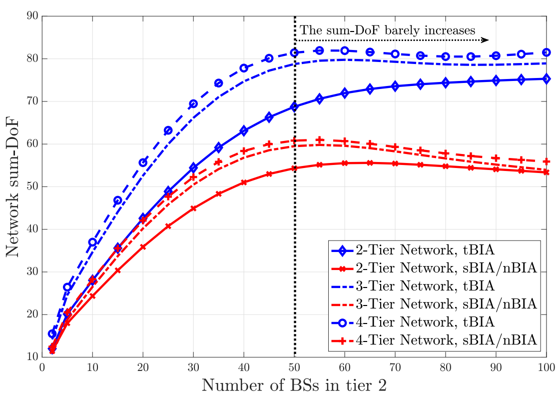


(b) Propagation index $\alpha = 3$.

Fig. 10. Evolution of the network sum-DoF as the density of BSs increases in a {2,3,4}-tier network. The tier 1 is composed of a single BS and the number of BSs in tiers 3 and 4 is 5 and 10 times the number of BSs in tier 2, respectively. The x-axis corresponds to the number of BSs in tier 2. $M_1 = 6$, $M_2 = 4$, $M_3 = 2$, $M_4 = 1$, $P_1 = 10P_2 = 100P_3 = 1000P_4$. $10^2$ users.

served by either the macro or the micro tier is depicted in Fig. 12(a). Considering that all the users of the network, i.e., $12 + 6 + 10 \times 3 = 48$ users, are served exclusively by a single tier composed of the macrocell using sBIA, a poor user-rate is achieved since the macrocell is overloaded. Introducing the micro tier, the achievable user-rate of the macro users is penalized considering the sBIA scheme, while the footprint of the microcell, i.e., the range in which a user obtains better rate than from the macrocell, covers less than 50 m. It can be also seen that avoiding the intracell interference through orthogonal resource allocation while not managing the inter-cell nor the inter-tier interference achieves low data rates in comparison with sBIA. Besides, the footprint of the microcell is even narrower. By using the proposed tBIA scheme, the microcell can operate subject to inter-tier interference from the macrocell. The users assigned to the micro tier improves their achievable rate considerably in comparison to the single tier case. Although providing a barely lower peak user-rate than sBIA, the tBIA scheme increases the footprint of the microcell (from point A to point B).

In Fig. 12(b), we analyze the rate achieved by a user connected to at least one femtocell regarding the position of the femtocell in the considered scenario. The distance between femto BS and femto user is fixed at 10 m. Since we consider a random deployment of 10 femtocells, the user can be categorized as private or shared. It is interesting to remark that the femto user can cancel the inter-tier interference from the macrocell, from the microcell or both. In this case, until the point A the femto user is limited just by interference from the macrocell, and therefore, the femtocell can implement tBIA as belonging to tier 2 interfered by the macrocell (tier 1). Within the points C and D the tBIA scheme provides greater user-rate canceling both tiers. In other words, the tBIA guarantees a spectral efficiency of 1 bit/sec/Hz for a footprint of the femtocell equal to 10 m even if the user receives a strong interference from two tiers. Interestingly, between the points D and E, canceling only the interference from the microcell provides the best user-rate. Beyond the point E, the best user-rate is obtained treating the inter-tier interference as noise. Furthermore, managing only the intracell interference using orthogonal resource allocation in each femtocell achieves

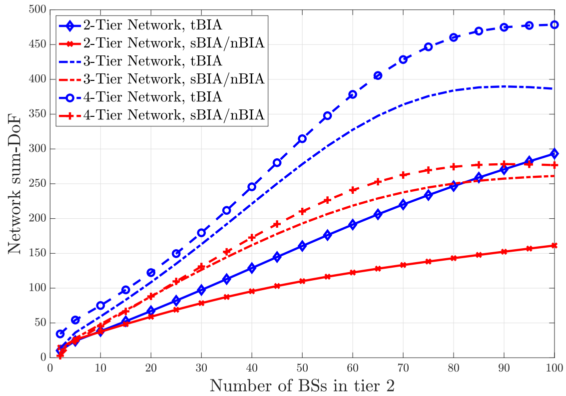


(a) Propagation index $\alpha = 2$

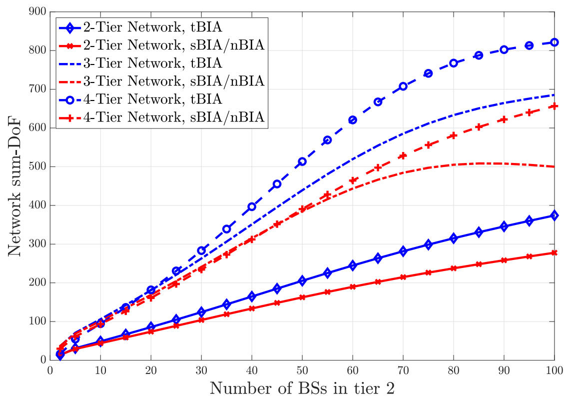


(b) Propagation index $\alpha = 3$

Fig. 11. Evolution of the network sum-DoF as the density of BSs increases in a {2,3,4}-tier network. The tier 1 is composed of a single BS and the number of BSs in tiers 3 and 4 is 5 and 10 times the number of BSs in tier 2, respectively. The x-axis corresponds to the number of BSs in tier 2. $M_1 = 6$, $M_2 = 4$, $M_3 = 2$, $M_4 = 1$, $P_1 = 10P_2 = 100P_3 = 1000P_4$. $10^4$ users.

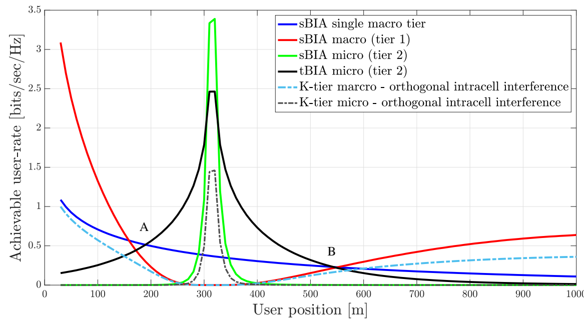


(a) User-rate for macro/micro users (tier 1 and tier 2)

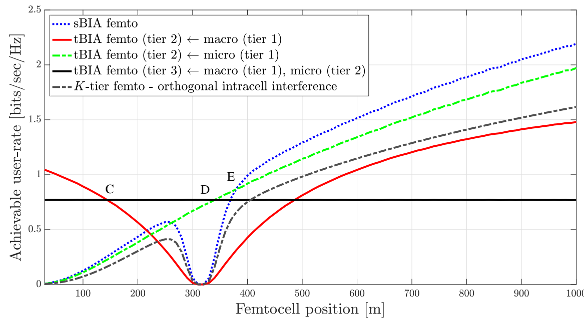


(b) User-rate for femto users (tier 3)

Fig. 12. Achievable user-rate for a three-tier cellular network.

lower user-rates than other solutions based on BIA.

## VIII. Conclusions

In this work, we analyze the impact of equipping users with reconfigurable antennas for interference management in $K$-tier networks without CSIT. An alternative BIA scheme is proposed for managing the inter-tier interference assuming that the tiers implement any BIA scheme. The DoF region for $K$-tier networks without CSIT is derived. After that, it is demonstrated that the proposed scheme reaches this region when selecting proper BIA schemes in each tier. Furthermore, simulation results show that the proposed scheme obtains greater DoF than other BIA strategies for $K$-tier networks and improves the user-rate subject to inter-tier interference.

## References

[1] A. Ghosh, N. Mangalvedhe, R. Ratasuk, B. Mondal, M. Cudak, E. Visotsky, T. A. Thomas, J. G. Andrews, P. Xia, H. S. Jo, H. S. Dhillon, and T. D. Novlan, "Heterogeneous cellular networks: From theory to practice," *IEEE Communications Magazine*, vol. 50, no. 6, pp. 54–64, 2012.

[2] M.-S. Alouini and A. Goldsmith, "Area spectral efficiency of cellular mobile radio systems," *Vehicular Technology, IEEE Transactions on*, vol. 48, no. 4, pp. 1047–1066, Jul 1999.

[3] H. Dhillon, R. Ganti, F. Baccelli, and J. Andrews, "Modeling and analysis of $K$-tier downlink heterogeneous cellular networks," *IEEE Journal on Selected Areas in Communications*, vol. 30, no. 3, pp. 550–560, April 2012.

[4] A. K. Gupta, H. S. Dhillon, S. Vishwanath, and J. G. Andrews, "Downlink multi-antenna heterogeneous cellular network with load balancing," *IEEE Transactions on Communications*, vol. 62, no. 11, pp. 4052–4067, 2014.

[5] Y. Lin, W. Bao, W. Yu, and B. Liang, "Optimizing user association and spectrum allocation in hetnets: A utility perspective," *IEEE Journal on Selected Areas in Communications*, vol. 33, no. 6, pp. 1025–1039, 2015.

[6] D. Liu, L. Wang, Y. Chen, M. Elkashlan, K. Wong, R. Schober, and L. Hanzo, "User association in 5G networks: A survey and an outlook," *IEEE Communications Surveys Tutorials*, vol. 18, no. 2, pp. 1018–1044, 2016.

[7] T. D. Novlan, R. K. Ganti, A. Ghosh, and J. G. Andrews, "Analytical evaluation of fractional frequency reuse for heterogeneous cellular networks," *IEEE Transactions on Communications*, vol. 60, no. 7, pp. 2029–2039, 2012.

[8] A. Shojaeifard, K. A. Hamdi, E. Alsusa, D. K. C. So, J. Tang, and K. Wong, "Design, modeling, and performance analysis of multi-antenna heterogeneous cellular networks," *IEEE Transactions on Communications*, vol. 64, no. 7, pp. 3104–3118, 2016.

[9] I. Boukhedimi, A. Kammoun, and M. Alouini, "Coordinated SLNR based precoding in large-scale heterogeneous networks," *IEEE Journal of Selected Topics in Signal Processing*, vol. 11, no. 3, pp. 534–548, 2017.

[10] G. Liu, M. Sheng, X. Wang, W. Jiao, Y. Li, and J. Li, "Interference alignment for partially connected downlink MIMO heterogeneous networks," *IEEE Transactions on Communications*, vol. 63, no. 2, pp. 551–564, 2015.

[11] W. Liu, L. Tian, and J. Sun, "Interference alignment for MIMO downlink heterogeneous networks," *IEEE Access*, vol. 8, pp. 35 090–35 104, 2020.

[12] T. Gou, C. Wang, and S. A. Jafar, "Aiming perfectly in the dark-blind interference alignment through staggered antenna switching," *IEEE*

*Transactions on Signal Processing*, vol. 59, no. 6, pp. 2734–2744, 2011.
[13] C. G. Christodoulou, Y. Tawk, S. A. Lane, and S. R. Erwin, "Reconfigurable antennas for wireless and space applications," *Proceedings of the IEEE*, vol. 100, no. 7, pp. 2250–2261, 2012.
[14] M. Hasan, I. Bahceci, M. A. Towfiq, T. M. Duman, and B. A. Cetiner, "Mode shift keying for reconfigurable MIMO antennas: Performance analysis and antenna design," *IEEE Transactions on Vehicular Technology*, vol. 68, no. 1, pp. 320–334, 2019.
[15] M. Johnny and A. Vahid, "Exploiting coherence time variations for opportunistic blind interference alignment," *IEEE Transactions on Communications*, vol. 68, no. 10, pp. 6054–6069, 2020.
[16] B. Lee, N. Lee, W. Shin, and H. V. Poor, "Blind interference alignment with ISI: A new look at OFDM for $K$-user interference channels," *IEEE Transactions on Signal Processing*, vol. 68, pp. 4497–4512, 2020.
[17] Q. Yang, T. Jiang, N. C. Beaulieu, J. Wang, C. Jiang, S. Mumtaz, and Z. Zhou, "Heterogeneous semi-blind interference alignment in finite-SNR networks with fairness consideration," *IEEE Transactions on Wireless Communications*, vol. 19, no. 4, pp. 2472–2488, 2020.
[18] C. Wang, H. C. Papadopoulos, S. A. Ramprashad, and G. Caire, "Design and operation of blind interference alignment in cellular and cluster-based systems," in *IEEE Information Theory and Applications Workshop*, 2011, pp. 1–10.
[19] M. Morales-Cespedes, J. Plata-Chaves, D. Toumpakaris, S. A. Jafar, and A. Garcia Armada, "Blind interference alignment for cellular networks," *IEEE Transactions on Signal Processing*, vol. 63, no. 1, pp. 41–56, 2015.
[20] F. C. Kavasoglu, Y. Huang, and B. D. Rao, "Semi-blind interference alignment techniques for small cell networks," *IEEE Transactions on Signal Processing*, vol. 62, no. 23, pp. 6335–6348, 2014.
[21] M. Morales-Cespedes, J. Plata-Chaves, D. Toumpakaris, S. A. Jafar, and A. G. Armada, "Cognitive blind interference alignment for macro-femto networks," *IEEE Transactions on Signal Processing*, vol. 65, no. 19, pp. 5121–5136, Oct 2017.
[22] M. Morales-Cespedes, L. Vandendorpe, and A. G. Armada, "Degrees of freedom of 2-tier networks without channel state information at the transmitter," *IEEE Signal Processing Letters*, vol. 26, no. 2, pp. 382–386, Feb 2019.
[23] Y. Xu, G. Gui, H. Gacanin, and F. Adachi, "A survey on resource allocation for 5G heterogeneous networks: Current research, future trends, and challenges," *IEEE Communications Surveys Tutorials*, vol. 23, no. 2, pp. 668–695, 2021.
[24] O. L. A. Lopez, N. H. Mahmood, H. Alves, C. M. Lima, and M. Latva-aho, "Ultra-low latency, low energy, and massiveness in the 6G era via efficient CSIT-limited scheme," *IEEE Communications Magazine*, vol. 58, no. 11, pp. 56–61, 2020.
[25] S. Akoum, C. S. Chen, M. Debbah, and R. W. Heath Jr., "Data sharing coordination and blind interference alignment for cellular networks," in *IEEE Global Communications Conference, 2012. GLOBECOM 2012*, 2012, pp. 4273–4277.
[26] Y. Lu, W. Zhang, and K. B. Letaief, "Blind interference alignment with diversity in $K$-user interference channels," *IEEE Transactions on Communications*, vol. 62, no. 8, pp. 2850–2859, 2014.
[27] A. Adnan-Qidan, M. Morales Céspedes, and A. García Armada, "User-centric blind interference alignment design for visible light communications," *IEEE Access*, vol. 7, pp. 21 220–21 234, 2019.

**Máximo Morales-Céspedes** (S'10-M'15) was born in Valdepeñas, C. Real, Spain, in 1986. He received the B.Sc., and M.Sc., and Ph.D. degrees from the Universidad Carlos III de Madrid, Spain, in 2010, 2012, 2015, respectively, all in electrical engineering, with a specialization in Multimedia and Communications. In 2012 he was finalist of the IEEE Region 8 Student Paper Contest. From 2015 to 2017 he has been working as a postdoctoral fellow with the Institute of Information and Communication Technologies, Electronics and Applied Mathematics (ICTEAM) at Universite Catholique de Louvain. Currently, he is with the Department of Signal Theory and Communications, Universidad Carlos III de Madrid, Spain. He serves as Editor in IEEE COMMUNICATION LETTERS and has been TPC member for numerous IEEE conferences (VTC, Globecom, ICC and WCNC). His research interests are interference management, hardware implementations, MIMO techniques and signal processing applied to wireless communications.

**Luc Vandendorpe** (Fellow, IEEE) received the degree (summa cum laude) in electrical engineering and the Ph.D. degree from the Universite Catholique de Louvain (UCLouvain), Louvain La Neuve, Belgium, in 1985 and 1991, respectively. Since 1985, he has been UCLouvain. He is now a Full Professor with the Institute for Information and Communication Technologies, Electronics, and Applied Mathematics, UCLouvain. His research interests include digital communication systems and more precisely resource allocation for OFDM(A)-based multicell systems, MIMO and distributed MIMO, sensor networks, UWB-based positioning, and wireless power transfer. He is and has been a TPC Member for numerous IEEE conferences (VTC, Globecom, SPAWC, ICC, PIMRC, and WCNC). He was a Co-Technical Chair for the IEEE ICASSP 2006. He served as an Editor for Synchronization and Equalization of the IEEE TRANSACTIONS ON COMMUNICATIONS between 2000 and 2002, and as an Associate Editor of the IEEE TRANSACTIONS ON WIRELESS COMMUNICATIONS between 2003 and 2005, and the IEEE TRANSACTIONS ON SIGNAL PROCESSING between 2004 and 2006. He was the Chair of the IEEE Benelux joint chapter on communications and vehicular technology between 1999 and 2003. He was an elected member of the Signal Processing for Communications Committee between 2000 and 2005, and an elected member of the Sensor Array and Multichannel Signal Processing Committee of the Signal Processing Society between 2006 and 2008, and between 2009 and 2011. Luc Vandendorpe is a Fellow of the IEEE.

**Ana Garcia Armada** (S'96-A'98-M'00-SM'08) received the Ph.D. degree in electrical engineering from the Polytechnical University of Madrid in February 1998. She is currently a Professor at University Carlos III of Madrid, Spain, where she has occupied a variety of management positions (Head of Signal Theory and Communications Department, Vice-dean of Electrical Engineering, Deputy Vice-Chancellor of International Relations, among others). She is leading the Communications Research Group at this university. She has been visiting scholar at Stanford University, Bell Labs and University of Southampton. She has participated (and coordinated most of them) in more than 30 national and 10 international research projects as well as 20 contracts with the industry, all of them related to wireless communications. She is the co-author of eight book chapters on wireless communications and signal processing. She has published more than 150 papers in international journals and conference proceedings and she holds four patents. She has contributed to international standards organizations, such as ITU and ETSI, is member of the expert group of the European 5G PPP and member of the advisory committee 5JAC of the ESA as expert appointed by Spain on 5G. She has served on the editorial boards of Physical Communication (2008-2017), IET Communications (2014-2017), and IEEE Communications Letters (Exemplary Editor Award 2017 and 2018). She serves on the editorial board of and IEEE Transactions on Communications and IEEE Open Journal of the Communications Society. She has served on the TPC of more than 40 conferences and she has been/is part of the organizing committee of IEEE Globecom (2019, 2021 General Chair), IEEE Vehicular Technology Conference (VTC) Fall 2018, Spring 2018 and 2019 and IEEE 5G Summit 2017, among others. She was the Newsletter Editor of the IEEE ComSoc Signal Processing and Consumer Electronics Committee (2017-2018) and is now the Secretary of this committee (since 2019). She has been the Secretary of the IEEE ComSoc Women in Communications Engineering Standing Committee (2016-2017) and the Chair of this committee (2018-2019). She has received the Young Researchers Excellence Award, from University Carlos III of Madrid. She was awarded the third place Bell Labs Prize 2014 for shaping the future of information and communications technology. She received the Outstanding service award from the IEEE ComSoc Signal Processing and Communications Electronics (SPCE) technical committee in 2019 and from IEEE ComSoc Women in Communications Engineering Standing Committee in 2020. Her main interests are multi-carrier and multi-antenna techniques and signal processing applied to wireless communications.